OPTIC NERVE INTERGRITY FOLLOWING RETINAL INACTIVATION FOR THE
TREATMENT OF POST-CRITICAL PERIOD AMBLYOPIA

by

Nadia Rita Dicostanzo

Submitted in partial fulfilment of the requirements
for the degree of Master of Science

at

Dalhousie University
Halifax, Nova Scotia
June 2020

TABLE OF CONTENTS

LIST OF TABLES

LIST OF FIGURES

ABSTRACT

In animal models, monocular deprivation (MD) by lid closure mimics the effects of unilateral amblyopia in humans. In cats, inactivation of the fellow (non-deprived) eye, with intraocular administration of tetrodotoxin has recently been shown to promote significant recovery from the effects of MD at older ages when conventional occlusion therapy fails. In the current study, the optic nerves of cats subjected to retinal inactivation of the fellow eye were assessed for histopathological changes as a means of assessing the safety of this potential new therapy. We examined the optic nerves of cats that were subject to up to 10 days of monocular inactivation therapy in their right eye and compared them to their left, control eye, as well as to the optic nerves from a control group of cats reared binocularly. In order to determine the extent of ocular imbalance for animals subjected to unilateral retinal inactivation therapy, the left and right optic nerves from all animals were assessed for signs of degeneration. This included observing for alterations in neurofilament labelling to assess axonal integrity, selectively staining myelin with luxol fast blue to asses for modifications of the myelin sheath, Nissl staining to quantify glial cell density, and immunolabeling for glial fibrillary acidic protein to asses for signs of gliosis. Our study revealed no evidence of gross histopathological changes in any of the markers assessed, revealing a normal balance between the left and right optic nerves from all animals and across both the treatment groups. These results indicate that retinal inactivation treatment did not significantly alter the integrity of the optic nerve and may be a viable therapeutic option for the treatment of post-critical period amblyopia.

LIST OF ABBREVIATIONS USED

AMPA: α-amino-3-hydroxy-5-methyl-4-isoxazolepropionic acid
ATP: adenosine triphosphate
Calpains: calcium-activated neutral proteases
CCAC: Canadian Council on Animal Care
CNS: central nervous system
dLGN: dorsal lateral geniculate nucleus
EAE: experimental allergic encephalomyelitis
GABA: gamma-aminobutyric acid
GAD65: glutamic acid decarboxylase 65
GFAP: glial fibrillary acidic protein
Iba-1: ionized calcium-binding adapter molecule 1
LFB: luxol fast blue
LGN: lateral geniculate nucleus
LTD: long term depression
LTP: long term potentiation
MBP: myelin basic protein
MD: monocular deprivation
MOG: myelin oligodendrocyte glycoprotein
mRNA: messenger ribonucleic acid
MS: multiple sclerosis
NAION: non-arteritic anterior ischemic optic neuropathy
NF: neurofilament
NF-H: neurofilament - heavy
NF-L: neurofilament - light
NF-M neurofilament -medium
NMDA: N-methyl-D-aspartate
NR2A: NMDA receptor subunit 2-A
NR2B: NMDA receptor subunit 2-B
OD: ocular dominance
ODI: ocular dominance index
Olig2: oligodendrocyte transcription factor 2
ONH: optic nerve head
PBS: phosphate-buffered saline
RAPD: relative afferent pupillary defect
RGC: retinal ganglion cell
TTX: tetrodotoxin
UCLA: University Committee for Laboratory Animals
WD: Wallerian degeneration

ACKNOWLEDGEMENTS

Chapter 1: INTRODUCTION

1.1 - Amblyopia

Amblyopia is a visual disorder that results from the disruption of normal visual input during the critical period early in postnatal development (von Noorden and Campos, 2002). Amblyopia is estimated to affect approximately 2-3% of the general population and is the leading cause of unilateral childhood visual impairment (Buch et al., 2001; von Noorden and Campos, 2002; Wright, 2003). If the amblyogenic cause is not corrected early in life, the neural circuitry within the visual system will not develop normally and can produce a severe and intractable visual impairment and an increased potential for loss of the non-amblyopic eye (Rahi et al., 2002; Tommila and Tarkkanen, 1981; van Leeuwen et al., 2007). Amblyopia clinically manifests as a unilateral, or occasionally as a bilateral reduction in best-corrected visual acuity for which no organic cause can be found on ocular examination (McKee et al., 2003; von Noorden, 1985). Unilateral amblyopia can be caused by abnormal binocular interaction and/or visual deprivation resulting in unequal visual input to the brain (von Noorden, 1985). This results in anatomical and structural changes in the lateral geniculate bodies and visual cortex that are presumed to underlie the disorder (von Noorden and Crawford, 1992).

In humans, the critical period for visual plasticity is the time during which individuals are most susceptible to developing amblyopia and have the greatest ability to recover from its effects. The critical period generally peaks during the first 2 to 3 years of life and the ability to develop amblyopia and recover gradually decreases after this point until the child reaches visual maturity which occurs around 7 years of age (Holmes et al., 2011; Holmes and Levi, 2018; von Noorden and Crawford, 1979).

1

In the clinical setting, treatment and effective recovery from amblyopia are normally reserved for young children due to their heightened neuroplasticity, and their positive response to therapies. As plasticity wanes with age, response to therapy attenuates and poor recovery outcomes usually result from conventional treatment regimes (Holmes et al., 2011). The most common therapy used to treat amblyopia is by penalization of the non-amblyopic eye (fellow eye), usually in the form of occlusion by a patch, optically, or pharmacologically. These treatments impede or blur the retinal image to the dominant eye and force the use of the amblyopic eye, thereby promoting the recovery of neuronal connections serving the weaker eye. If instilled with compliance during the critical period, these therapies have been shown to be effective at reversing the effects of amblyopia (Loudon et al., 2002; Pediatric Eye Disease Investigator Group, 2002).

However, compliance with conventional therapies is relatively low, with almost half of amblyopic patients patching less than 75% of the prescribed hours regardless of the hours prescribed (Pediatric Eye Disease Investigator Group, 2002, 2003; Wang, 2015). Even with recent advances to objectively monitor compliance such as occlusion dose monitors, compliance remains low (Awan et al., 2005; Wallace et al., 2013). Several factors including psychosocial dynamics, adverse treatment side effects, patient age, severity of amblyopia, prescribed dosage, socioeconomic status, education, and parental stress may all play a role in the level of adherence to amblyopia treatments (Dixon-Woods et al., 2006; Loudon et al., 2009; Newsham, 2000; J. Wang, 2015).

Furthermore, even with adequate compliance, when traditional penalization therapies are instilled past the critical period they are no longer effective and yield little to no recovery (Holmes et al., 2011; Scheiman et al., 2005; C. Wu and Hunter, 2006).

1.2 - Animal models of amblyopia and the critical period

In animal models, monocular deprivation (MD) by lid suture mimics many of the effects of unilateral amblyopia by stimulus deprivation. The cat model, in particular, has been used for decades to show the effects of and recovery from MD given its anatomical similarities to the human visual system.

The findings of Hubel and Wiesel in the 1960s laid the groundwork for much of our current understanding about the development and plasticity of the brain. One of the pivotal findings from this influential work was the identification that many cells within the cat's primary visual cortex could be excited by visual stimuli from either eye (Hubel and Wiesel, 1962). The extent to which one eye can elicit these cortical cells based on their receptive field properties is known as ocular dominance (OD). In normal cats raised binocularly, either eye is able to by some degree stimulate the vast majority of these cortical cells (Freeman and Olson, 1982; Hubel and Wiesel, 1962,1963a). However, if MD is imposed during the critical period, a shift occurs in the responsiveness of the cortical neurons, such that the non-deprived eye is able to better excite previously binocular cells, while the deprived eye is able to elicit few cortical cells due to weakened and even lost synaptic connections (Blakemore and Van Sluyters, 1974; Rittenhouse et al., 1999; Wiesel and Hubel, 1963a). These dramatic effects are not as severe even given no pattern visual stimuli to either eye, imposed via binocular lid suture early in development (Blakemore and Van Sluyters, 1974; Hubel and Wiesel, 1965). Thus, the

3

extreme shift in ocular dominance is governed by the relative input between the two eyes, as activity dependant competition between the two eyes drives ocular dominance.

Physiological changes in response to MD are accompanied by anatomical changes in the striate cortex and dorsal lateral geniculate nucleus (dLGN). In the striate cortex of cats and monkeys reared binocularly, the inputs from the eye-specific layers of the LGN serving the two eyes are segregated into ocular dominance columns of relatively equal size (LeVay et al., 1980; Shatz and Stryker, 1978).With the introduction of MD during the critical period the ocular dominance columns receiving input from the deprived eye shrink, and the columns receiving input from the non-deprived eye expand (LeVay et al., 1980; Shatz and Stryker, 1978). This dynamic shift is not only dependant on activity but also the quality of sensory input. Furthermore, the cortical changes induced my MD give rise to the anatomical modifications in the dLGN. Such that a significant reduction in neuronal soma sizes can be detected in the dLGN layers that receive projections from the deprived eye in both cats and monkeys subject to MD during the critical period (Guillery and Stelzner, 1970; Hubel et al., 1977; Wiesel and Hubel, 1963b).

The effects of MD are directly related to the capacity for neural plasticity, with animals aged to maturity exhibiting little to no effect of visual deprivation (Hubel and Wiesel, 1970; Olson and Freeman, 1975). Plasticity, therefore, decreases with age and the effects of MD are observed only during the critical period when plasticity is high and neural connections can be readily modified. In cats, the critical period occurs between the 4th and 6th week of age (Hubel and Wiesel, 1970; Olson and Freeman, 1975). During this period, one week of MD can cause a near complete shift in ocular dominance

4

towards the non-deprived eye, leaving the deprived eye able to activate few if any cortical neurons (Hubel and Wiesel, 1970). The sensitivity to MD is known to decline following the 6th week and is negligible past the 3rd month of age (Hubel and Wiesel, 1970; Olson and Freeman, 1975).

The capacity for recovery from the effects of MD coincides with this period of sensitivity. In kitten subject to MD followed by a period of reverse suturing (opening the previously deprived eye and suturing the non-deprived eye) during the critical period, a complete shift in ocular dominance towards the initially deprived eye is produced (Hubel and Wiesel, 1970). However, if MD is imposed in young kittens and reverse suturing performed following the critical period, ocular dominance is unaffected and the primary visual cortex cells are still driven almost exclusively by the initial non-deprived eye (Blakemore and Van Sluyters, 1974; Movshon, 1976). Meaning that earlier intervention yields greater recovery, with typical recovery strategies imposed on visually mature animals having no beneficial effect.

1.3 - Mechanisms of cortical plasticity

There exist several mechanisms that underlie the heightened plasticity experienced during the critical period that enables the drastic physiologic and structural modifications that occur with MD. It is important to note that much of our current understanding into the molecular and cellular mechanisms of plasticity comes from rodent models. Unlike cats and primates, rodents do not have segregated anatomical ocular dominance columns, rather, they possess cells of variance ocular dominance distributed throughout the cortex in a 'salt-and-pepper' pattern with the majority of cells

preferring stimuli from the contralateral eye (Ohki and Reid, 2007). Nevertheless, due to the ease of gene-targeting therapies rodents provide an essential model for neuroplasticity research.

It has been proposed that the plasticity experienced during the critical period is the result of perfectly balanced excitatory and inhibitory cortical transmission that only occurs once in life (Hensch, 2005). Therefore, manipulation of either excitatory or inhibitory circuitry would affect the extend of deprivation and recovery (Hensch and Fagiolini, 2005).

Gamma-aminobutyric acid (GABA) is the chief inhibitory neurotransmitter in the central nervous system (CNS). In mice, reducing the release of GABA from the presynaptic neuron via deletion of the glutamic acid decarboxylase 65 (GAD65) gene produces an insensitivity to the effects of MD during the critical period such that the predictable shift in OD towards the non-deprived eye does not occur (Hensch et al., 1998). Restoration of plasticity can be achieved with diazepam (a GABA agonist), as treatment of GAD65 knockout mice with diazepam infusions during MD enables the ocular dominance shift towards the non-deprived eye (Hensch et al., 1998). Therefore, inhibitory transmission is essential for the experience-dependent plasticity that occurs during the critical period.

Furthermore, the maturation of inhibitory circuitry may delineate, the heightened synaptic plasticity observed at the peak of the critical period, as $GABA_A$ receptor composition is developmentally regulated. Prior to the onset of the critical period GABA α3 is the dominant subunit expressed by GABAergic receptors in the visual cortex (Chen et al., 2001). However, around the peak of the critical period a shift occurs such that the

α1 subunit becomes dominant. The maturation of GABAergic circuitry is experience-dependant such that, dark rearing, which prolongs the critical period, delays the shift from α3 to α1 GABA$_A$ receptor subunit composition (Chen et al., 2001). Furthermore, it has been shown that with the introduction of a GABA agonist, the critical period can be started prematurely (Fagiolini and Hensch, 2000), however, this premature critical period initiation will not occur without the presence of the α1 subunit (Fagiolini et al., 2004). Demonstrating the essential role of GABAergic inhibitory mechanisms and receptor maturation for the commencement of the critical period.

In addition to inhibitory mechanisms that enable plasticity, over the past several decades much has been learned about the excitatory circuitry within the visual system and the mechanisms that enable the strengthening and weakening of synaptic connections. Based on the foundations of Hebbian synaptic modifications, such that synaptic pathways are strengthened the more they fire together (Hebb, 1949). Whenever synchronous presynaptic neurons elicit a postsynaptic response, the synapses are strengthened and therefore stabilize. This is thought to occur due to modifications of glutamate-gated-ion channels on the postsynaptic neuron, specifically α-amino-3-hydroxy-5-methyl-4-isoxazolepropionic acid (AMPA) and N-methyl-D-aspartate (NMDA) receptors. The NMDA receptors are voltage-gated and require not only glutamate (the primary excitatory neurotransmitter in the CNS) to allow access of calcium ions into the postsynaptic neuron, but they also require the postsynaptic membrane to depolarize in order to remove the receptors magnesium block (Nowak et al., 1984). Strong NMDA receptor activation can strengthen synaptic transmissions, also known as long term potentiation (LTP). The influx of calcium ions from activated NMDA receptors triggers

biochemical mechanisms that increase synaptic efficacy in part by increasing the amount of AMPA receptors on the post-synaptic terminal (Lüscher and Malenka, 2012). AMPA receptors aid in depolarizing the postsynaptic membrane allowing for easier activation of the post-synaptic cell (Barry and Ziff, 2002; Bear et al. 2016; Lüscher and Malenka, 2012), and further strengthening synaptic connections.

Conversely, long term depression (LTD), is the weakening of synaptic connections. If the postsynaptic neuron is elicited infrequently the synaptic strength is decreased and the cellular mechanisms that enable postsynaptic firing are less efficient, further weakening synaptic connections (Bear et al. 2016; Lüscher and Malenka, 2012). The long-term consequences of LTD are synaptic elimination and the retraction of the presynaptic neuron (Coleman et al., 2010; Piochon et al., 2016). In monocularly deprived animals, the synaptic connections receiving input from the non-deprived eye are strengthened whilst the deprived eye receives significantly lower levels of input and synaptic connections are therefore weakened.

Importantly, the crossover point between synaptic weakening (LTD) and synaptic strengthening (LTP) is not fixed and is modified based on the history of postsynaptic activation changing the threshold for LTP or LTD to occur (Kirkwood et al., 1996). A period of increased activity increases the threshold for LTP and consequently promotes LTD, whereas a period of decreased activity lowers the modification threshold and promotes LTP (Kirkwood et al., 1996; Philpot et al., 2007).

It has been proposed that this shift in the modification threshold is likely due to a change in NMDA receptor composition and function. NMDA receptors are composed of obligatory NR1 subunits along with a combination of NR2A-D subunits which can alter

receptor properties (McBain and Mayer, 1994). Similar to GABAergic receptors, the NMDA receptor composition undergoes an experience dependant shift in the relative subunit composition, such that NR2B is predominant in young animals at the beginning of the critical period, and NR2A becomes predominant between the peak and end of the critical period, increasing the NR2A/NR2B ratio (Nase et al., 1999). Reduced NR2A expression changes the LTD/LTP threshold such that, some stimulation frequencies that would normally cause LTD instead generate LTP (Cho et al., 2009). Furthermore, in dark reared animals (which are known to have a delayed critical period) there is a shift in the in the LTP/LTD threshold, and LTP is promoted, accompanied by a decrease in the NR2A/NR2B ratio. When animals are re-exposed to light the threshold shifts to promote LTD, and the NR2A/NR2B ratio increases rapidly (Chen and Bear, 2007; Cooper and Bear, 2012; Quinlan et al., 1999).

The change in NMDA receptor subunit composition also causes changes in the kinetics of the NMDA receptor influencing the relative calcium influx and modifying the likelihood of either LTP or LTD. Immature NMDA receptors (containing NR2B subunits) have slower opening and closing kinetics, and in turn, remain open for longer allowing for an increased calcium influx and an added likelihood for LTP to occur. Conversely, NR2A mature receptors show much faster opening and closing kinetics, and less calcium influx is enabled, therefore promoting LTD (Quinlan et al., 1999; Santucci and Raghavachari, 2008).

Furthermore, similar to the requisite role of GABAergic transmission to produce MD, blocking NMDA receptor function likewise prevents the effect of MD during the

9

critical period (Bear et al., 1990). Thus, excitatory transmission is also required to elicit the experience dependant plasticity that occurs during the critical period.

Although several other molecular and cellular mechanisms are expected to be involved in determining the levels of visual system plasticity, the balance between excitatory and inhibitory mechanisms likely plays a key role in the plasticity that is required for MD and therefore, recovery from its effects. Understanding the mechanisms that may influence the levels of plasticity in the visual system allows for the potential to manipulate the critical period and possibly enable access to limited plasticity resources in the adult brain.

1.4 - Post-critical period recovery

Researchers have been exploring novel therapies that may enable post-critical period recovery due to the limited treatment window in which traditional therapies have proven to be effective. In humans, binocular treatments of amblyopia for post-critical period recovery such as dichoptic video game therapies have become increasingly popular in current research. In a recent multi-centre randomized clinical trial by Holmes et al. in 2019, a binocular therapy in the form of an iPad game (DigRush) which reduces contrast to the fellow non-amblyopic eye was compared to optical correction alone in children ages 7-12 years of age. The results of this study demonstrated that following 8 weeks of dichoptic therapy no significant benefit in visual acuity nor stereoacuity was produced compared to controls (Holmes et al., 2019). Notwithstanding, several small case series and single-center randomized trials have shown positive results using dichoptic therapies in both visual acuity and stereoacuity (Hess et al., 2010; Kelly et al., 2016; Li et al., 2013). However, many of these have failed to gain wide acceptance amongst

clinicians due to limitations such as clinically insignificant outcomes, subjects with previously treated amblyopia, a lack of a normal control group, and treatment availability to only those with binocular vision which is reserved for anisometropic amblyopes and strabismic amblyopes with peripheral fusion. Currently, there is no widely accepted clinical therapy used to treat amblyopia in visually mature humans that achieves significant recovery.

In cats, significant post-critical period recovery had until recently, only been effective with enucleation or severe trauma to the fellow eye. This radical treatment proved to be successful in reversing the anatomical, physiological and behavioural effects of MD in the deprived eye long after the critical period in which traditional occlusion would yield negligible effects (Cragg et al., 1976; Kratz and Spear, 1976; Smith et al., 1978). This effect has also been demonstrated in humans. Several case studies have shown notable recovery in adults in cases of unilateral amblyopia in which extensive disease, severe trauma, and/or enucleation occurs in the fellow eye, and remarkably, visual acuity in the previously amblyopic eye recovers (Klaeger-Manzanell et al., 1994; Wang and Shuba, 2014).

This phenomenon gives rise to the theory that perhaps traditional therapies are not potent enough to access waning plasticity resources. Therefore, it is possible that more efficacious therapies could access lower levels of plasticity resources in older amblyopes to promote superior recovery outcomes compared to mainstay treatments, optimistically, without detrimental effects to the fellow eye. In a recent study, a novel therapy that temporarily pharmacologically inactivates the fellow eye was able to reverse the effects of MD in cats after the critical period (Duffy et al., 2018).

1.4.1 - Tetrodotoxin for post-critical period recovery

Recovery from MD in visually mature animals has recently been shown in cats through the administration of small amounts of intraocular tetrodotoxin (TTX). TTX is a neurotoxin that functions as a reversible voltage-gated sodium channel blocker. TTX inhibits action potentials by blocking the passage of sodium ions into the cell but does not interfere with critical cell functions such as axoplasmic transport. When injected into the vitreous chamber of a cat eye, it nearly abolishes all retinal ganglion cell (RGC) activity for approximately 48 hours (Duffy et al., 2018; Fong et al., 2016) after which visual ability is believed to return to normal. In a recent study by Duffy et al. (2018), monocularly deprived kittens were aged to a stage of visual maturity that have little to no capacity for recovery from the effects of MD via traditional therapies. These monocularly deprived animals had their deprived eye opened and were treated with intraocular injections of TTX in their fellow eye. Remarkably, this therapy resulted in a complete anatomical recovery from the effects of MD which was demonstrated by a full recovery of soma sizes within the deprived layers of the dLGN, amazingly, without detriment of the neurons serving the inactivated eye (Duffy et al., 2018).

It has been proposed that the mechanisms that underlie this unprecedented recovery may derive from a shift in the modification threshold based on previous cortical activity. Such that, abolishing retinal input from the stronger fellow eye leaves only the weak previously deprived eye as a source of cortical input (Cooper and Bear, 2012; Duffy et al., 2018). Theoretically, this would shift the modification threshold promoting LTP rather than LTD, and allowing the synaptic connections from the deprived eye to strengthen. In addition to, or alternatively, fellow eye inactivation may enable access to

limited plasticity resources allowing for recovery in visually mature animals. (Cooper and Bear, 2012; Duffy et al., 2018).

Considering the exciting therapeutic potential of retinal inactivation as a treatment for amblyopia in older animals, the current study aims to assess the safety of TTX injections as they relate to ocular pathology, specifically as it relates to the optic nerve. A major advantage of examining the optic nerve for signs of pathology and degeneration is that the complete output from the RGCs can be accessed from a single cross-section of the nerve. Additionally, in select ocular diseases such as glaucoma, it has been shown that axonal degeneration occurring in the optic nerve may precede the loss of RGC bodies in the retina (Calkins, 2012; Howell et al., 2013; Nakazawa et al., 2006). Thus, examining the optic nerve may reveal earlier signs of pathology and be a more sensitive measure of degeneration.

1.5 - Optic nerve

1.5.1 - Optic nerve structure and organisation

The optic nerve is the second cranial nerve and comprises retinal ganglion cell axons, glial cells (astrocytes, oligodendrocytes, and microglia), connective tissues, and blood vessels. The optic nerve can be divided into 4 parts each with their own distinct anatomical features: 1) the optic nerve head (ONH), which represents the portion of the optic nerve that is contained within the globe and holds the lamina cribosa; a sieve-like structure that acts as a barrier to maintain the intraocular pressure and allow the passage of RGC axons and blood vessels; 2) the intraorbital section, which represents the optic nerve as it leaves the globe (retrolaminarly) and travels back to the orbital apex. This

section measures approximately 10mm in length in the average adult cat (Evans and Jeffery, 1992), and is surrounded by three meningeal layers; the pia, arachnoid, and dura matter. Oligodendrocytes begin to myelinate axons in the intraorbital section of the optic nerve. This myelination occurs gradually over the first 1-1.5mm of optic nerve retrolaminarly, after which point the axons become uniformly myelinated (Blunt et al., 1965); 3) the intracranial portion, which represents the optic nerve as it exits the orbit through the optic canal and travels back and medially to the optic chiasm which is approximately 4mm in length in the adult cat (Evans and Jeffery, 1992); and finally, 4) the optic chiasm, in which the nasal fibres of the optic nerves decussate. After this point, the optic nerve becomes the optic tract and the fibres travel back to the thalamus, in particular the LGN in which the majority of the axons terminate. The total length of the optic nerve from the ONH to the chiasm of the average adult cat measures approximately 14mm (Evans and Jeffery, 1992).

Axons of the mammalian optic nerve are organised into fascicular bundles. In cats, the number and organization of these fascicles depends on the location of the optic nerve. Within the ONH there is a high degree of organization and the axons are organized meticulously into many fascicular bundles (Evans and Jeffery, 1992). These axons are unmyelinated and the extra-fascicular spaces are reserved for astrocytes, blood vessels, and connective tissues (Jeffery et al., 1995; Triviño et al., 1996). As you travel back from the ONH into the intraorbital section of the optic nerve this fascicular structure becomes less meticulous and the number of fascicles declines. With this, astrocytes begin to depart from their compartmentalized extra-fascicular space and are found both within and surrounding the fascicular bundles (Triviño et al., 1996). The fascicular structure is

regained in the orbital canal and then almost completely lost before the nerve decussates at the optic chiasm (Evans and Jeffery, 1992). In both cats and humans, it has been proposed that this change in structural organization along the optic nerve pathway may be an adaptation to protect the nerve from mechanical damage. Such that the locations with a higher degree of organization and well defined extra-fascicular matrices containing connective tissues are at locations that are more exposed to maneuvers from extraocular movements (Jeffery, 1996; Jeffery et al., 1995).

1.5.2 - Blood supply

In primates, the central retinal vessels arise from a singular central retinal artery and vein. The central retinal artery enters the optic nerve posteriorly to the lamina cribosa and enters the ONH centrally parallel with the central retinal vein (May, 2008).

Unlike in primates, the optic nerves of cats do not contain a single central artery and vein. Rather, the retinal vascular supply of the cat comes from 4-5 arteries and 4-5 veins that send branches to the retina via the lateral portion of the ONH (Henkind, 1966; Wong and Macri, 1964). Additionally, a more significant and robust complex of vessels arising from the pia matter that surrounds the optic nerve, supply the optic nerve of the cat. This pial septa exists in primates, however, it is less extensive and contains fewer pial vessels (May, 2008).

1.5.3 - Axons

The axons of the optic nerve contain axoplasm (axonal cytoplasm) that is surrounded by the axolemma (plasma membrane of the axon). The axolemma is similar in structure to the cell membrane of the cell body, and it contains numerous ion channels which maintain the membrane potential and allow for depolarizing activity (Strominger et

15

al., 2012). The axoplasm contains the cytoskeleton which is made up of neurofilaments (NFs), microtubules, and microfilaments which play an essential role in maintaining axonal structure and coordinating various functions for maintenance. The cytoskeleton is not a fixed structure but will undergo changes during development, growth and after injury (Strominger et al., 2012).

NFs are the most commonly expressed intermediate filament and are composed of three distinct subunits: Neurofilament light NF-L, Medium NF-M, and Heavy NF-H based on their molecular mass (Lee and Cleveland, 1996). NFs within the axons of the optic nerve are highly phosphorylated and play the most important role in maintaining the axonal structure, shape, and quality (Petzold, 2005).

1.5.4 - Myelin

The myelin sheath is a lipid heavy envelope that surrounds and protects the axons of the CNS. This electrically insulating sheath plays a key role in axonal transport, maintaining axonal structure and function, and aids in protecting axons from inflammatory processes (Stassart et al., 2018). Most importantly, fully functioning myelin is required for the rapid conduction of action potentials along the length of axons known as saltatory transduction which is enabled by myelin's unique formation of regular interruptions at the nodes of Ranvier (Strominger et al., 2012).

1.5.5 - Glial cells

Neuroglia (glia) which were first described by Virchow in 1864 as "nerve glue" are the supportive cells of the CNS, providing structural and metabolic support to the nerve fibres (Strominger et al., 2012). Glial cells, which have been identified within the

optic nerve can be further subdivided into macroglia (oligodendrocytes, and astrocytes) and microglia.

1.5.5.1 - Oligodendrocytes

Oligodendrocytes are spherical cells with small regular round nuclei and numerous processes that form and maintain the myelin sheaths that envelops and protects axons within the CNS (García-Cabezas et al., 2016). The processes of a single oligodendrocyte have the capacity to extend to more than 50 axons (Felten et al., 2016). In addition to providing the myelin sheath that protects and insulates axons, oligodendrocytes have also been found to be involved in the metabolic support of axons by providing lactate for axonal mitochondrial adenosine triphosphate (ATP) generation (Saab et al., 2013). As well as aiding in regulating axonal growth and accumulation of NFs (Sánchez et al., 2000).

1.5.5.2 - Astrocytes

Astrocytes are star-shaped cells with an ovoid nucleus and smooth nuclear envelope (García-Cabezas et al., 2016). They possess an extensive network of long processes that can extend entire lengths of the optic nerve (Butt et al., 1994). These processes aid in creating a barrier between axons and the pial septa (Triviño et al., 1996). Astrocytes also provide essential support for neuronal functions including homeostatic maintenance, metabolic, and physical support (Stromiger et al., 2012).

Additionally, astrocytes play an important role in the scarring and repair process of the CNS. When faced with acute CNS trauma, ischemia, inflammation, and neurodegenerative diseases, astrocytes take on a reactive form propelling a cascade of events known as reactive astrogliosis (Stromiger et al., 2012). This process is key in

17

both disease progression and the recovery process. Reactive astrocytes proliferate, undergo cellular hypertrophy, regulate inflammatory processes, and form glial scars (Sofroniew, 2016). Additionally, It has also been proposed that astrocytes are capable of acting as phagocytic cells in the presence of CNS trauma and can aid macrophages in the process of clearing cellular debris (Jones et al., 2013; Nguyen et al., 2011).

1.5.5.3 - Microglia

Microglia are small irregular shaped cells, their nuclei can be round, elongated, comma-shaped, or poly-lobular and their cytoplasm may contain several inclusion bodies (García-Cabezas et al., 2016). Microglia are classified as cells of the immune system due to their response to foreign bodies, brain injury, and inflammation. When introduced with injury, microglia take on an activated form and are recruited to the site of injury to function as phagocytes to remove cellular debris (Strominger et al., 2012).

1.6 - Models of nerve degeneration

In order to determine the integrity of the optic nerve, understanding the mechanisms by which nerve structures change and degenerate in the presence of pathology is essential. There exist several models of neuronal degeneration that exhibit and follow select response patterns in the presence of a pathological or toxicological insult in the CNS. Many neuropathies can be classified into either axonal degeneration (Wallerian and dying-back neuropathies) in which the degeneration of myelin is secondary to axonal loss, or demyelinative degeneration in which axonal degeneration is secondary to loss of its protective myelin sheath.

1.6.1 - Axonal degeneration

Wallerian degeneration (WD) was first described by Augustus Waller in 1850 who made the observation that following nerve transection the distal portion of the nerve underwent progressive degeneration while the proximal portion remained intact (Waller and Owen, 1851). In this type of degeneration, when an axon is transected or crushed its distal part undergoes a series of changes leading to its complete structural and chemical degradation.

One of the first changes that occurs in WD is the swelling of the axolemma. This is followed by the granular disintegration of the cytoskeleton, in which the cytoskeletal components including NF proteins are broken down, resulting in the fragmentation of the axon (Griffin et al., 1995). The mechanisms underlying this process are thought to be regulated by an increase in intracellular calcium which triggers calpains (calcium-activated neutral proteases) to break down the cytoskeletal components (Dubový et al., 2013). Damage to the axon triggers a formulaic response from surrounding glial cells; astrocytes and microglia are recruited to the site of injury and are stimulated to release pro-inflammatory cytokines. Oligodendrocytes undergo apoptosis and axons are subsequently demyelinated (Warden et al., 2001). Phagocytic cells clear the axonal and myelin debris and degenerated axons are replaced by reactive glial cells, forming a glial scar (Griffin et al., 1995). Although previously reserved for degeneration that ensued after axonal transection or crush, several other disorders of the CNS have been linked with WD such as stroke (Thomalla et al., 2005), and Alzheimer's disease (Serra et al., 2010).

Dying-back neuropathies were first described by John Prineas in 1969. It depicts a degeneration of the axon which begins at the distal end and progresses retrogradely towards the cell body (Prineas, 1969). This type of degeneration has been found to underlie a multitude of chronic neurologic diseases including toxin-induced neuropathies, nutritional disorders, metabolic disorders, uraemia, and certain carcinomas (Schaumburg and Spencer, 1979; Sumner and Asbury, 1975). The cellular mechanisms underlying dying-back neuropathies are similar to WD and therefore, may also be referred to as Wallerian-like degeneration (Coleman, 2005; Griffin et al., 1995). Recently it has been proposed that both WD and dying-back neuropathies are likely to be related and that the axonal degeneration will undergo similar processes regardless of the type of pathological insult (Coleman, 2005; M.-S. Wang et al., 2000).

These models of axonal degeneration have been found to occur in the optic nerve following excitotoxic injury, which is a mechanism involved in several diseases of the CNS including glaucoma and retinal ischemia (Osborne et al., 2004). In a study by Saggu et al. (2010) the effects of induced excitotoxic injury to the retina were explored in the distal and proximal portions of the optic nerve. 72 hours post-injury, they reported evidence of Wallerian-like degeneration which involved axonal swelling, cytoskeletal disintegration, and granulation of cytoskeletal components. 7 days post-injury, extensive invasion of astrocytic processes, and signs of demyelination which were more prominent at the distal end of the nerve in comparison to the proximal end were identified (Saggu et al., 2010). Wallerian and Wallerian-like degeneration have also been identified in the optic nerve following optic nerve crush injury (Cottee et al., 1991), enucleation (Khan, 2004; Ludwin, 1990), and animal models of glaucoma (Crish et al., 2010).

1.6.2 - Segmental demyelination

Segmental demyelination, unlike WD and dying-back neuropathies, is reserved for neuropathies in which the myelin sheath is degenerated while the axons remain relatively intact or degrade secondary to the loss of the myelin sheath (Seil, 1982; Wisniewski and Bloom, 1975). Demyelination is mainly a consequence of oligodendrocyte apoptosis and can occur through many mechanisms including genetic defects, inflammatory processes, autoimmune reactions, and trauma (Alizadeh et al., 2015). This type of degeneration has been described in several disorders including, diphtheritic neuropathy (Hadfield et al., 2000), post-infectious encephalomyelitis (Johnson and Griffin, 1987), Guillaume barre syndrome (Prineas, 1981), lead poisoning (Dyck et al., 1980) and multiple sclerosis (MS) (Wisniewski and Bloom, 1975). In demyelinating disorders, the demyelination is typically accompanied by inflammatory processes, and reactive astrogliosis (Popescu et al., 2013).

This model of segmental demyelinative disease is often reported in the optic nerve most prominently with optic neuritis, which is a demyelinating disorder of the optic nerve that is frequently associated with MS and neuromyelitis optica. The demyelinative consequences of these disorders are believed to be facilitated by acute inflammatory processes followed by a subsequential axonal degeneration leading to severe and sometimes irreversible neurological damage (Pau et al., 2011; Wu et al., 2015).

1.7 - Markers of optic nerve degeneration

Regardless of the classification or type of degeneration that occurs following a pathologic insult, several changes to the nerve structure and its supportive cells can be observed in the presence of pathology. Changes to the axonal cytoskeleton, myelin, and

the neuroglia that support them can all be indicative of a pathological insult. Thus, when examining the integrity of the optic nerve and determining if there exist signs of pathology, directly looking at these structures and their cellular markers that respond in a formulaic pattern to pathological changes will aid in determining the integrity of the optic nerve following injections of TTX.

1.7.1 - Axonal degeneration

The degradation of cytoskeletal components of the axon is one of the first observable changes in axonal degeneration. In particular, NF subunits, which play a key role in the pathogenies of axonal degeneration and dysfunction and are commonly used as markers for optic nerve fibre degeneration and loss (Petzold, 2005). Several well-documented animal models that mimic clinical pathologies such as retinal ischemic injuries (Renner et al., 2017; Song et al., 2003), glaucoma (Bordone et al., 2017), non-arteritic anterior ischemic optic neuropathy (Miller et al., 2014; Zhang et al., 2010) and enucleations (Marques et al., 2003) use decreases and/or changes to NF structure to demonstrate the axonal degeneration that ensues from these models of disease. One of the most common ways to observe the integrity of NF is by immunohistochemical techniques to label NF proteins, specifically phosphorylated NF, which is readily found in axons as it aids in creating the robust cytoskeletal structure. As NF labelling decreases one can assume loss of cytoskeletal structure and axonal degeneration have occurred (Marques et al., 2003; Petzold, 2005; Renner et al., 2017).

1.7.2 - Demyelination

Demyelination of axons is a hallmark of neuronal disease, as demyelination of axons can occur secondary to axonal degeneration or be the primary cause of disease

(Stassart et al., 2018). Researchers have examined myelin to asses optic nerve integrity and to demonstrate the presence of pathology when myelin is lost or develops structural abnormalities in the optic nerve in a multitude of diseases. The identification of myelin can be done in many ways including immunohistochemical labelling of myelin basic protein (MBP) (Renner et al., 2017) and identifying structural changes through the myelin lamellae with electron microscopy (Marques et al., 2003). However, one of the most common and simplest ways to observe the organization and abundance of myelin in the optic nerve is with the use of Luxol Fast Blue (LFB). LFB selectively stains myelin and has been used readily by researchers to demonstrate pathological changes in the optic nerves of experimental animal models of many ocular and optic nerve diseases such as retinal ischemic injury (Renner et al., 2017), MS (Castoldi et al., 2020), and glaucoma (Bordone et al., 2017) in these models decreases in staining intensity demonstrates a loss of myelin in the optic nerve.

1.7.3 - Gliosis

Gliosis is a term used to describe the changes in glial cells that occur in the CNS in response to a pathological insult. Glial cells in the optic nerve have been shown to perform predictable responses to pathology. Oligodendrocytes will typically undergo apoptosis and consequently demyelination of optic nerve axons will ensue (Bradl and Lassmann, 2010). This has been demonstrated in many ocular diseases including optic neuritis (Bradl and Lassmann, 2010), retinal ischemic injury (Renner et al., 2017) ocular hypertension, experimental models of glaucoma (Nakazawa et al., 2006) and models of acute optic nerve injury in cats (Yu and Zhang, 2011).

In contrast, in the presence of optic nerve disease, microglia will take on a reactive form and are recruited to the site of injury to perform the phagocytic removal of cellular debris. This increase in microglial cell number by proliferation and/or recruitment of phagocytes is known as microgliosis. The increase in microglial expression in the optic nerve has been demonstrated in cases of optic nerve crush injury (Bordone et al., 2017), retinal ischemic injuries (Ahmed et al., 2017; Renner et al., 2017) and in experimental models of glaucoma in which the extent of microglial activation has been shown to be proportional to the severity of optic nerve degeneration (Bosco et al., 2015).

In addition to changes in oligodendrocytes and the activation of microglial cells, changes in astrocytic function, expression, and localisation have been used to demonstrate the presence and extend of disease for decades. This biological change in astrocytes in the presence of pathology is known as astrogliosis and is a hallmark of degeneration in the CNS and optic nerve.

1.7.3.1 - Astrogliosis

Astrocytes take on a reactive form in the presence of CNS injury. Reactive astrocytes show an altered expression of many genes and an upregulation of glial fibrillary acidic protein (GFAP) (Hol and Pekny, 2015). GFAP is a principle intermediate filament in the astrocytes cytoskeleton which provides structural support to astrocytes and their processes (Eng and Ghirnikar, 1994). In the presence of CNS injury astrocytes proliferate and undergo cellular hypertrophy, this is characterized by a rapid increase in GFAP (Eng and Ghirnikar, 1994). Reactive astrocytes are capable of modulating several important features of CNS injury, which aid in both the recovery and degenerative

24

processes of CNS disease. These mechanisms include the formation of glial scars that comprise mainly of reactive astrocytes. These scars function to isolate damaged tissue and restrict inflammation and neurotoxic mediators to the site of injury, thus, promoting less acute inflammatory damage (Bush et al., 1999; Mayo et al., 2014). Reactive astrocytes also play a key role in the active repair of the blood-brain barrier and are able to modulate blood vessel diameter (Sofroniew, 2016). Although the role of reactive astrocytes and the formation of glial scars in the acute phases of CNS disease may be beneficial, in chronic disease such as MS, reactive astrocytes may promote sustained inflammation and in turn, increase neurodegeneration (Mayo et al., 2014).

Increases in GFAP has been used extensively as a biomarker for disease in the optic nerve for several disorders including experimental models of glaucoma (Gallego et al., 2012), human primary open angle glaucoma (Hernandez et al., 2008), optic nerve crush injury (Bordone et al., 2017; Stankowska et al., 2018), non-arteritic anterior ischemic optic neuropathy (Miller et al., 2014) and has been established as an early biomarker for neurotoxicity (O'Callaghan, 1991).

In addition to increases in GFAP, reactive astrocytes and their astrocytic processes may also further infiltrate axonal fascicles in the presence of disease, and the nerve bundles may show greater disorganization of their cytoarchitecture (Marques et al., 2003). Thus, localization of astrocytes and their processes may also be used as a marker for degeneration. Immunohistochemical labelling of GFAP can provide an overall understanding of the extent of optic nerve and CNS injury with increases in GFAP intensity labelling demonstrating higher degrees of pathological processes.

25

The unprecedented post-critical period recovery from the effects of MD that were demonstrated by Duffy et al. (2018) by retinal inactivation of the fellow eye showcased the exciting therapeutic potential of TTX as a possible treatment for post-critical period amblyopia. Translation of this therapy or similar retinal inactivation treatments relies on the safety of the therapy. Thus, ensuring no detrimental effects were produced in the fellow eye is crucial.

The current study aims to assess the safety of intravitreal TTX injections by examining the optic nerves of monocularly deprived animals subjected to multiple inactivation treatments for gross signs of histopathology. Several well documented histological features were assessed to determine if signs of pathology were present in the optic nerves. This included observing for axonal loss or degeneration by assessing the staining intensity of phosphorylated NF, evaluating for modifications to myelin by assessing the staining intensity of luxol fast blue, and examining for glial cell changes which involved estimating the overall glial cell density in optic nerve cross-sections and examining the intensity of GFAP immunofluorescent staining.

CHAPTER 2: MATERIALS AND METHODS

2.1 - Experimental design

Seventeen kittens reared from birth in a closed colony at Dalhousie University were used for this study. All procedures described below were approved by the Dalhousie University Committee for Laboratory Animals (UCLA) and followed the Canadian Council on Animal Care (CCAC) Guidelines. Details regarding the rearing history of the animals are presented in Table 1. In summary, the kittens were divided into 3 experimental groups:1) a control group (Normal) in which kittens were reared binocularly for approximately 6-14weeks (n=4), two of which received intraocular injections of a vehicle solution of citrate buffer in their right eye that paralleled the dosage and timeline of injections in the treatment groups; 2) an experimental group (RETTX), in which kittens were monocularly deprived in their left eye at the peak of the critical period (postnatal day 30) for 6 -18 weeks, this was followed by opening the deprived eye and 8-10 days of retinal inactivation by intraocular injections of TTX in the fellow eye (n=7); 3) an experimental group (RETTX+BV), in which 6-15 weeks of monocular deprivation of the left eye was followed by 10 days or retinal inactivation by intraocular injections of TTX in the fellow eye and then up to 20 days of unobstructed binocular vision (n=6).

2.2 - Experimental procedures

2.2.1 - Monocular deprivation

For all animals in the experimental groups, monocular deprivation was performed on postnatal day 30 under general anesthesia using 3-4% isoflurane in oxygen. The animal's body temperature was maintained using a heating pad at 37°C. The upper and

27

lower palpebral conjunctivae of the left eye were sutured closed using vicryl suture material, followed by closure of the left eyelids with silk suture material. producing a two-layer occlusion, depriving the left eye of all pattern visual stimuli. The lid closure procedure lasted about 15 minutes after which animals were administered subcutaneous Anafen as a means of postoperative analgesia and were given topical ophthalmic Alcaine (proparacaine hydrochloride) for local anesthesia. A broad-spectrum topical antibiotic (1% Chloromycetin) was applied to the closed lids to prevent infection. Animals were monitored daily to ensure animal health and to confirm proper lid closure was maintained.

2.2.2 - Retinal inactivation

Following the period of MD, animals from the experimental groups were anesthetized with 3-4% gaseous isoflurane in oxygen and body temperature was maintained using a heating pad at 37°C. The left eyelids were opened, at which point the right eye received an intravitreal injection of TTX (3mM dissolved in citrate buffer; 0.5 μl / 100-gram body weight). Injections were administered through a small puncture made in the sclera located at the ora serrata using a sterile 30-gauge needle. Using a surgical microscope, the measured volume of TTX solution was dispensed into the vitreous chamber using a sterilized Hamilton syringe with a 30-gauge needle (point style 4) that was positioned through the original puncture and about 5-10 mm into the chamber angled away from the anterior chamber. The total volume of TTX was dispensed slowly, and when complete the needle was held in place for about a minute before it was retracted. Following intraocular injection, a topical antibiotic (1% Chloromycetin) and local anesthetic (Alcaine) were applied to the eye to prevent post-injection complications. To

achieve 10 days of inactivation, animals received five injections, one every 48 hours, as a single dose of TTX administered intravitreally eliminates visual responses for at least 48 hours (Duffy et al., 2018; Fong et al., 2016). For each injection, the original puncture site was used to avoid having to make another hole. During the period of inactivation, a visual assessment was employed to confirm effective retinal inactivation. The absence of a pupillary light reflex, as well as the lack of visuomotor behaviors such as visual placing reflex, visual startle, and the ability to track a moving laser spot were verified. These assessments were made while vision in the non-injected eye was briefly occluded with an opaque contact lens.

2.2.3 - Histology

Animals from the RETTX group were sacrificed two days after the final TTX injection, and animals from the RETTX +BV group were sacrificed following the period of binocular vision. Animals were anesthetized with isoflurane (5% in oxygen) prior to receiving a lethal dose of sodium pentobarbital (euthanyl; 150 ml/kg) delivered intraperitoneally. Animals were then transcardially perfused with 150 ml of phosphate-buffered saline (PBS) followed by an equal volume of 4% paraformaldehyde dissolved in PBS. Immediately after perfusion the eyes with their respective optic nerves were removed and immersed in a PBS solution containing 30% sucrose to cryoprotect tissues for sectioning. The optic nerves from each eye were cut just distal to the globe and an approximate 5mm piece of optic nerve was collected for processing. Optic nerves that were less than 5mm were cut as proximally to the globe as possible and the maximum amount of optic nerve was used for sectioning. Following cryoprotection, the meningeal

layers surrounding the optic nerves were removed and the optic nerves were sliced into cross-sections of 50μm thickness using a freezing microtome (Leica SM2000R; Germany).

Cross-sections to be labeled for neurofilament were mounted on a single glass slide and allowed to dry overnight. A solution containing the mouse monoclonal antibody targeting NF (1:1000 dilution; SMI-32; BioLegend, USA) was placed on the slide thoroughly covering all cross-sections. Sections were left in the primary antibody solution for 2 hours and then washed with PBS. A solution containing the secondary antibody (1:500 dilution; Goat anti-mouse Alexa 488; 115-585-003; Jackson Immunoresearch, USA) was placed on the slide covering all cross-sections completely for one hour and then washed with PBS a second time. The slide was then coverslipped with a curable antifade mounting medium (Prolong Gold; Thermo Fisher, USA).

Cross-sections to be stained for myelin were mounted on glass slides and allowed to dry overnight. The optic nerve sections from all animals were mounted on a single slide and reacted at one time. Sections were hydrated in distilled water for 3 minutes, then immersed in luxol blue stain (ab150675; abcam, USA) for two hours at 60 °C. The slide was then rinsed in distilled water and differentiated by submerging the sections in a 0.05% Lithium carbonate solution. The cross-sections were then dehydrated by immersing them in a graded series of ethanol concentrations. The cross-sections were cleared using Histo-clear (DiaMed Lab Supplies Inc.; Mississauga, ON, CAN) and Permount was used to coverslip the sections (Fisher Scientific; Canada).

Cross-sections to be stained for Nissl substance were mounted on a single glass slide and allowed to dry overnight. Sections were immersed in a graded series of ethanol concentrations, placed in a solution of 0.1% cresyl violet acetate dye in distilled water for 5 minutes, and then immersed in the graded series of ethanol a second time for differentiation. Sections were cleared using Histo-clear (DiaMed Lab Supplies Inc.; Mississauga, ON, CAN) and Permount was used to coverslip the sections (Fisher Scientific; Canada).

Sections to be labelled for GFAP were mounted on a single glass slide and allowed to dry overnight. The slide was immersed in a solution containing Triton X-100 (1:500 dilution) for 1 hour in order to permeabilize the sections and improve antibody access to the GFAP antigen. Cross-sections were then washed with PBS and immersed in a solution containing the rabbit-anti-GFAP antibody (1:1000 dilution; ab7260; abcam, USA) for 2 hours. The cross-sections were washed again with PBS and were immersed in a solution containing the secondary antibody (1:500 dilution; Goat anti-rabbit Alexa 594; 111-585-003; Jackson Immunoresearch, USA) for 1 hour. The slide was then washed with PBS for a final time and coverslipped with a curable antifade mounting medium (Prolong Gold; Thermo Fisher, USA).

2.2.4 - Quantification

All measurements in this study were taken blind to the animal condition as well as to which eye was being examined. Measurements were taken using a BX-51 compound microscope (Olympus; Markham, Ottawa, Canada) fitted with an Infinity3S-1UR microscopy camera (Lumenera Corporation, Ottawa, ON), which allows for the

transmission of the microscope image to a computerized stereology software suite (newCast; VisioPharm, Denmark). For the assessment of glial cell density, a 60X oil immersion objective was used, and glial cells were individually counted from 5-8 randomly selected counting frames of 30245.8μm^2 each. Only glial cells (which were made visible with Nissl stain) with a clearly defined nucleolus were counted, and a marker was placed on the counted cell to ensure each cell was only counted once during quantification. The approximate glial cell density per mm^2 of each optic nerve cross-section was estimated by dividing the number of cells by the total area from which cells were counted. To compare results from the right and left nerves an ocular dominance index (ODI) was calculated by subtracting the sum of the right optic nerve measurements from the sum of the left (inactivated) optic nerve measurements and then dividing the result by the sum of the left optic nerve measurements, and finally, multiplying by 100 so that the final product of the metric indicated the percentage difference between left and right optic nerves (Duffy et al., 2018).

Ocular Dominance Index :

((left optic nerve – right optic nerve) / left optic nerve) x 100

The quantification of the fluorescence produced by NF and GFAP immunolabelling and the staining intensity of luxol fast blue dye were all quantified following the procedure described below. Five images at 60X magnification with an area of 69000 μm^2 from a predetermined location on each optic nerve cross-section (top, bottom, left, right, and centre) were captured. From the 5 images, an average grayscale

value for each of the optic nerve cross-sections was calculated using the ImageJ software (Schneider et al., 2012). For the quantification of fluorescence intensity for NF and GFAP, clearly defined fascicular bundles were outlined and the grayscale values of only the fascicular spaces were used to determine the average gray value for each optic nerve. For the quantification of luxol staining intensity, the entire area of each image was used to calculate the average gray value. These values were used to calculate the ocular dominance index to compare the average staining intensities of NF, GFAP, and Luxol between the left and right optic nerves.

2.3 - Statistical analysis

For each measurement, the extent of difference between the left and right optic nerve within each animal condition was evaluated using the ocular dominance index that indicated the extent of difference for each animal between the two eyes for each of the markers assessed. Statistical assessments were performed on the raw data (Tables 1) with a two-tailed Kruskal-Wallis nonparametric analysis of variance using Dunn's multiple comparisons test. A Kruskal-Wallis statistic with Dunn's multiple comparisons test was also used to evaluate differences in the ocular dominance indices between groups. All statistical analyses and data visualizations were conducted using the GraphPad Prism software (version 8.0.0 for Mac OS X, GraphPad Software, San Diego, California USA, www.graphpad.com).

CHAPTER 3: RESULTS

3.1 - Neurofilament

Examination of immunolabelling of NF from optic nerve cross-sections of both control and experimental groups revealed distinct fluorescent axonal fascicles and opaque dark extra-fascicular spaces. For normal animals reared binocularly, NF labeling intensity, and distribution in the left and right optic nerves appeared balanced (Figure 1A). NF labelling intensity across sections from animals in the RETTX experimental group that received MD followed by retinal inactivation of the fellow eye revealed comparable levels of NF labelling intensity in left and right optic nerves (Figure 1B) which was indistinguishable from controls. Moreover, NF labelling intensity from left and right optic nerve cross-sections in the second experimental group (RETTX+BV) which received up to 20 days of binocular vision following retinal inactivation showed comparable staining intensities (Figure1C) and were likewise similar to controls.

The ODIs as determined by the quantification of NF intensity revealed minor differences between left and right optic nerves as ODIs were close to zero for controls and both treatment groups (Figure 1D). No significant difference was found between the ODIs of treatment groups and controls (H=[3] = 0.76, p=0.71; Dunn's multiple comparison test: p > 0.05). Neurofilament labeling intensity was not significantly different between the left and right optic nerves across groups (H=[6] = 6.22, p = 0.28; Dunn's multiple comparison test: p > 0.05), nor was there a difference in labelling intensity between the experimental groups and normal controls (Dunn's multiple comparison test: p > 0.05). These results demonstrate a relatively equal incidence of cytoskeletal NF from control and inactivated eyes.

3.2 - Myelin

Examination of optic nerve cross-sections stained to reveal myelin with LFB of both control and experimental groups revealed a consistent staining pattern across all optic nerve cross-sections. Examination of optic nerve sections stained with luxol from the normal group revealed a uniformity in staining intensity and staining pattern between the left and right optic nerves (Figure 2A). Luxol staining intensity across sections from animals in the RETTX experimental group revealed comparable levels of staining intensity and consistency in left and right optic nerves (Figure 2B) which was indistinguishable from controls. Additionally, luxol staining intensity from left and right optic nerve sections in the RETTX+BV experimental group showed comparable staining intensities and uniformity between right and left nerves (Figure 2C) and were likewise similar to controls.

These observations were paralleled with the results of our quantification of luxol staining intensity which revealed balanced values measured from the left and right optic nerves in control animals and treatment groups, indicated by ODI values close to zero (Figure 2D), with no difference in ODIs between treatment groups and controls (H=[3] = 0.95, p = 0.64; Dunn's multiple comparison test: p > 0.05). There was no statistical difference in luxol staining intensity measurements between the left and right optic nerves for the control group or either of the two treatment groups (H=[6] = 7.70, p = 0.17; Dunn's multiple comparison test: p > 0.05). likewise, there was no statistical difference in luxol staining intensity between the optic nerves of our control and treatment groups

(Dunn's multiple comparison test: p > 0.05). These results are consistent with their being an equal level of myelination in control and inactivated eyes.

3.3 - Nissl

Glial cell density was assessed by examining Nissl stained sections of optic nerve which revealed distinct glial cell bodies and their darkly stained nucleolus. layers of glial cells were arranged throughout the optic nerve cross-sections with a slightly higher density within septa surrounding the fascicular spaces. There was no obvious change in uniformity nor cell density between left and right nerves of controls (Figure 3A), and left and right optic nerves from both experimental groups (Figure 3 B and C) which appeared consistent between treatment groups and controls.

Quantification of Nissl-stained cell density was consistent with our qualitative observations; ODI calculations were balanced between the left and right nerves across conditions (Figure 3D), with no difference in ODIs between treatment groups and controls (H=[3] = 0.67, p = 0.74; Dunn's multiple comparison test: p > 0.05). There was no significant difference in cell density between left and right nerves across conditions (H=[6] = 1.86, p = 0.86; Dunn's multiple comparison test: p > 0.05), nor between the nerves of controls and the treatment groups (Dunn's multiple comparison test: p > 0.05). Indicating equal glial cell densities in controls and inactivated eyes.

3.4 - GFAP

Examination of optic nerve cross-sections immunolabeled for GFAP revealed bright astrocytic cell processes extending evenly through fascicular spaces. GFAP labeling intensity and distribution appeared balanced between the left and right optic

nerves for animals in the normal group (Figure 4A). GFAP labelling intensity across

sections from animals in the RETTX experimental group revealed comparable levels of

GFAP labelling intensity in left and right optic nerves (Figure 4B) which was similar to

controls. Furthermore, GFAP labelling intensity from left and right optic nerve sections

in the RETTX+BV experimental group showed comparable staining intensities between

left and right optic nerves (Figure 4C) and were likewise comparable to controls.

This was supported by our measurements of fluorescence intensity that was

balanced between left and right optic nerve for controls and both experimental groups

(Figure 4D) with no significant difference in the ODIs between treatment groups and

controls (H=[3] = 0.49, p = 0.79; Dunn's multiple comparison test: p > 0.05). Across the

three groups studied, there was no statistical difference in GFAP immunofluorescence

between left and right optic nerves (H=[6] = 3.71, p = 0.59; Dunn's multiple comparison

test: p > 0.05), nor was there a statistical difference between optic nerves of controls and

the optic nerves from the treatment groups (Dunn's multiple comparison test: p > 0.05).

demonstrating comparable levels of GFAP in optic nerves of experimental groups and

controls.

CHAPTER 4: DISCUSSION

Following the demonstration that intraocular injections of TTX in the fellow eye facilitates post-critical period recovery from the effects of MD in cats (Duffy et al., 2018). The current study sought to determine the integrity of the optic nerve following intraocular injections of TTX. Several anatomical characteristics that produce well documented and observable changes in terms of histopathology in the optic nerve were assessed. This included modifications to neurofilament, myelin, and glial cells. We observed no obvious histopathological changes in the optic nerves of animals that underwent retinal inactivation in any of the markers assessed in this study. Results demonstrated a balance in NF immunolabeling, myelin staining intensity, glial cell density, and GFAP fluorescence intensity between the left and right optic nerve of all animals, as well as optic nerves from treatment groups being similar to controls. These results are consistent with the conclusion that retinal inactivation does not significantly alter the anatomical integrity of the optic nerve.

4.1 - Consequences of TTX on the development of the retina and optic nerve

Comparable to the results of this study, TTX imposed on immature animals does not seem to alter optic nerve axonal density. However, when imposed prenatally by intracranial perfusion, TTX may alter the optic nerve structure. During prenatal and early postnatal development many neurons within the CNS undergo naturally occurring cell death including retinal ganglion cells and their respective axons. In the cat, approximately 65% of retinal ganglion cells die between embryonic days 44 and 56, this period of rapid cell death is followed by a slow decline in RGCs until approximately 1 month postnatally

(Williams et al., 1986). In a study by Friedman and Shatz (1990), the effects of intracranial TTX infused just prior to the rapid phase of cell death (embryonic day 42) for up to two weeks were assessed. Following 2 weeks of intracranial TTX, the optic nerve axonal density in the nerves of TTX treated animals were not different from controls. However, the ultrastructure of the optic nerve was found to be abnormal, displaying increased glial cell infiltration and a loss of axonal fascicular structure compared to controls when examined by electron microscopy (Friedman and Shatz, 1990). They suggested that this change in optic nerve structure may have been caused by a high level of intracranial TTX, or that intracranial TTX may have a direct effect on the development of glial cells and prenatal glial cell migration from the diencephalon (Friedman and Shatz, 1990).

Conversely, in study a by O'Leary et al. (1986) rat pups, were subject to repeated monocular injections of intraocular TTX every second day for up to 14 days starting at postnatal day zero. The optic nerve axonal density was found to be similar in TTX treated eyes and controls, demonstrating a comparable loss of optic nerve axons (O'Leary et al., 1986). However, in contrast to the structural findings of Friedman and Shatz (1990), the optic nerves from the TTX treated eyes appeared normal and were indistinguishable from controls with comparable myelinated fibres, axons, and glial cells when examined by electron microscopy (O'Leary et al., 1986).

Likewise, in the current study, the qualitative observations revealed, optic nerves from TTX treated eyes that were indistinguishable from controls, furthermore the fascicular structure of the optic nerve was maintained and optic nerves from inactivated eyes had similar fascicular patterns to their fellow eye as well as to normal controls.

These observations were supported by an even distribution of glial cells between treated and control optic nerves and similar staining intensities of luxol, NF, and GFAP across all optic nerve cross-sections.

Although retinal inactivation via intraocular injection of TTX does not appear to alter the optic nerve structure or retinal ganglion cell axonal density, it has been shown that retinal inactivation imposed on post-natal immature cat retinas does affect the regular pattern of adjacent ON-OFF retinal ganglion cell pairs. In normal postnatal development, approximately 20% of α-ganglion cell death occurs in the central retina (Jeyarasasingam et al., 1998). In a study by Jeyarasasingam et al. (1998), monocular retinal inactivation introduced on postnatal day 9 for 3 weeks did not affect the magnitude of normal cell death. However, retinal inactivation imposed on immature retinas did change the distribution pattern of ON and OFF ganglion cells. Thus, the formation of the normal retinal mosaic pattern is disrupted by retinal inactivation imposed early in postnatal life, but retinal ganglion cell density is not (Jeyarasasingam et al., 1998). Therefore, intracranial or intravitreal TTX imposed prenatally or in early post-natal life may disrupt some the developing structures in the retina and optic nerve and may produce negative effects if used in immature animals.

4.2 - Consequences of retinal inactivation in mature animals

Though retinal inactivation and intracranial TTX imposed in prenatal and early postnatal development may cause abnormalities in the development of the retina and optic nerve, the effects of intraocular TTX in older animals beyond postnatal development seems to be inconsequential. In a study by Wong-Riley and Riley (1983), 10

cats received up to 6 weeks of retinal inactivation by intraocular injection of TTX. The retinas of these animals appeared grossly normal with no signs of trauma, nor any indication of pathology (Wong-Riley and Riley, 1983). Decreases in the level of cytochrome oxidase (a marker for metabolic activity in the CNS) were exhibited in the layers of the LGN receiving inputs from the inactivated eye and the visual cortex. Cytochrome oxidase levels returned to normal when afferents were restored as the effects of retinal inactivation wore off (Wong-Riley and Riley, 1983). These effects were comparable to those of Wong-Riley and Carroll (1984) who demonstrated that unilateral retinal inactivation caused entirely reversible decreases in cytochrome oxidase levels in the macaque striate cortex, LGN, and retina (Wong-Riley and Carroll, 1984). In accordance with the previous study on cats, the retinas remained histologically intact and were similar to controls, RGCs were also shown to maintain axonal transport. Thus, apart from temporary decreases in oxidative metabolism along the visual pathway of inactivated eyes, the effects of retinal inactivation by TTX in mature animals appears to be unremarkable.

These histological conclusions are supported by the behavioural results in cats that demonstrate a full recovery of normal visual acuity following 4 days of retinal inactivation with binocular administration of TTX (Fong et al., 2016). These findings are further reinforced by the return to normal visual acuity in adult humans following intraocular injections of lidocaine, which is a short-lasting sodium channel blocker often used in surgical procedures. In a case series, lidocaine was inadvertently injected into the eyes of 3 adult human patients (Lincoff et al., 1985). The first, during a procedure to remove a lower lid tumour in which the sclera was penetrated just anterior to the equator

and 0.5cc of 2% lidocaine-epinephrine was injected into the globe at which point the pupil immediately dilated. Visual acuity was deemed no light perception in the superior field and count fingers in the inferior field with no pupillary response for several hours. 16 hours after the injury the pupillary response was normal and visual acuity returned to 20/20 (Lincoff et al., 1985). The two other case studies from this series involved similar amounts of intraocular lidocaine and demonstrated a complete loss of visual acuity and a lack of a pupillary response in the injected eye. The second case also achieved a return to normal visual acuity. However, in the 3rd patient, vision was impaired by a dense scotoma which involved fixation. The authors reported that the field defect was likely the result of a subretinal hemorrhage that occurred from the injection site damaging the retina (Lincoff et al., 1985). The authors of this study also supplemented these findings with animal studies involving adult cats and rabbits who underwent intraocular lidocaine injections. No significant retinal damage, nor signs of toxicity were found in any of the animal retinae analysed (Lincoff et al., 1985).

Furthermore, another study revealed no evidence of retinal toxicity following intracameral administration of lidocaine in a patient who previously underwent a pars plana lensectomy and vitrectomy (Hoffman and Fine, 1997). Subsequent to lidocaine injection, complete loss of vision was reported as well as a significant relative afferent pupillary defect (RAPD). Several hours after administration of lidocaine the patient made a full visual recovery, without an RAPD implying that the inactivation did not elicit gross ocular pathology nor meaningful damage along the optic nerve (Hoffman and Fine, 1997).

These case studies indicate that when a substance with a similar mechanism of action to TTX is injected into the eyes of adult humans, no discernible consequences to the injected eye have been reported, with the exception of trauma induced by the injection itself. Therefore, it is possible that a similar substance, such as TTX may not cause any determent to the injected eye given the injection is carefully and intentionally administered.

4.3 - Effective retinal inactivation

In the current study, no obvious histopathological changes were detected in the optic nerves of animals that underwent retinal inactivation treatments in any of the markers assessed. One might speculate that the lack of histopathological changes observed were due to ineffective administration of TTX that resulted in weak or absent retinal inactivation. However, all animals that received intravitreal TTX were assessed for functional characteristics that are associated with proper retinal inactivation that have been used in a multitude of studies to demonstrate effective administration of intraocular TTX. This includes the absence of a pupillary light reflex in the injected eye (Duffy et al., 2018; Fong et al., 2016; M. Wong-Riley and Carroll, 1984; Wong-Riley and Riley, 1983), and a lack visuomotor behaviours when using the inactivated eye (Duffy et al., 2018; Fong et al., 2016). These characteristics are indicative that retinal inactivation was administered and performed effectively. Furthermore, some of the animals in the current study were subjects in a previous study by Duffy et al. (2018), in which retinal inactivation of the fellow eye was demonstrated to promote anatomical recovery from the effects of MD past-the critical period (Duffy et al., 2018). These results are assumed to

43

have only been demonstrable given effective administration of retinal inactivation treatments.

4.4 - The effects of MD on the retina and optic nerve

The animals in this study that were subject to retinal inactivation were monocularly deprived prior to the subsequent retinal inactivation treatment, as they were a part of a previous or current investigation to examine inactivation as a potential therapy for deprivation-induced amblyopia. It could be speculated, that the balance reported for all measures between right and left eye in the experimental groups could be the result of balanced pathology in the left eye caused by MD and the right eye caused by TTX. However, MD does not appear to alter retinal or optic nerve characteristics in animal studies. Retinal ganglion cell density and retinal ganglion cell soma sizes are unaltered even when MD is imposed for up to 7 years in cats (Spear and Hou, 1990). Additionally, no difference was found in retinal ganglion cell number, nor in their axonal conduction velocities in RGCs of monocularly deprived cats following over 1 year of MD in comparison to controls (Sherman and Stone, 1973). Moreover, no pathological findings suggesting optic nerve atrophy were reported in the optic nerves of the amblyopic eyes of rhesus monkeys who had undergone MD by lid suture for up to seven years (von Noorden, 1973). When compared, the optic nerves of amblyopic eyes were not different from optic nerves of non-deprived eyes, with neither showing abnormalities or signs of atrophy (von Noorden, 1973).

In the current study equal pathological findings between right and left optic nerves in the experimental groups is unlikely as the results of this study demonstrated that there was no difference between either eye of the experimental groups and the eyes of the

normal controls in which all animals were reared binocularly with no previous MD. Indicating, that the optic nerve characteristics examined in the present analyses were not significantly altered by MD.

4.5 - Timing of histopathological modifications in the optic nerve

In the current study, the effects of 10 days of retinal inactivation via intraocular injection of TTX in the optic nerve were examined in two treatment groups: the first two days after the final injection of TTX, and the second up to 22 days following the final injection. One potential limitation of this study is that possible negative effects of TTX and corresponding histopathological changes may not have been evident after the allotted time. The timing at which evidence of optic nerve degeneration is observable varies in the literature depending on the animal model, type of pathological insult that occurs, instrumentation used, as well as which marker of pathology is being examined.

In rodent models, the optic nerve degeneration that occurs following an acute increase in intraocular pressure by ischemic injury supports the current timeline of this study. The axonal degeneration that ensued after retinal ischemic injury in a mouse model was apparent in the optic nerve just 3 days after injury, with evident decreases in NF immunolabelling. This decrease was further educed 7 days post-injury, along with a visible decrease in immunostaining of myelin basic protein (Song et al., 2003). Furthermore, in a study by Renner et al. (2017) a rat model of retinal ischemic injury was conducted. 21 days following the injury, NF in the optic nerves showed a structural distortion with shortened axons and a loss of structural integrity compared to control optic nerves. Luxol fast blue staining was also reduced demonstrating the demyelinative

45

effect of the injury (Renner et al., 2017). Astrocytic cell changes were evaluated by assessing GFAP expression as well as GFAP positive area of optic nerve longitudinal sections. Although no significant differences were found for GFAP positive area in ischemic nerves, a structural disorganisation of astrocytes was observed and a significant increase in GFAP expression at the mRNA level was evident 21 days post-injury (Renner et al., 2017). In addition to these findings, a study that investigated the consequences of experimental acute glaucoma in owl monkeys was also able to report signs of degeneration shortly after injury (Lampert et al., 1968). With the use of electron microscopy, just 12 hours following the procedure apparent granular disintegration of the nerve was evident, after 24 hours, there existed evidence of swollen astrocytic processes and phagocytosis of cellular debris, 72 hours following the procedure, reactive astrocytes with densely packed glial filaments were appreciated (Lampert et al., 1968).

In animal models of non-arteritic anterior ischemic optic neuropathy (NAION), which is an isolated stroke to the optic nerve, the time course of axonal degeneration is also comparable. In a rodent model of NAION, the axonal loss that ensued following the procedure was evident just 7 days post-injury with decreases in NF immunolabelling. Severe axonal damage and loss along the entire optic nerve and optic nerve head were demonstrated 14 days post-injury (Zhang et al., 2010). Moreover, in a primate model of NAOIN, the optic nerves of rhesus monkeys showed marked decreases in NF immunolabeling just 7 days after injury (Salgado et al., 2011).

In demyelinative disorders such as experimental allergic encephalomyelitis (EAE) which is an experimental model of MS, the time course for demyelination to occur may be delayed. Castoldi et al. (2020) observed the demyelinative properties of the disease in

46

a rat model of EAE at 56 days and furthermore at 70 days post-immunization, with optic

nerves showing significant decreases in LFB staining. Axonal loss and demyelination in

this model of EAE seemed to follow relatively similar timelines as neither LFB staining

nor NF immunolabeling were significantly decreased 21 days post-immunization and

both showed significant decreases after 56 days (Castoldi et al., 2020). Additionally, in

adult marmoset monkeys with induced EAE signs of demyelination were not observable

until 26 days post-immunization (Diem et al., 2008). Notwithstanding the delayed

demyelinative properties of EAE, other signs of histopathology such as astrogliosis may

be observable prior to demyelination of the optic nerve. In a study by shields (1998), just

12 days post-immunization an increased number of glial cells and intense GFAP

immunoreactivity were observed in a rat model of EAE (Shields et al., 1998).

      With direct mechanical damage to the optic nerves such as in optic nerve

transections, optic nerve crush injuries, and enucleations more severe and almost

immediate histopathological changes can be observed. In rats that underwent bilateral

enucleations, initial NF loss, and disturbances to the myelin structure could be observed

just 48 hours post-enucleations (Marques et al., 2003). Similarly, initial signs of

degeneration could be observed in rabbits who underwent monocular enucleations just 24

hours after the procedure (Khan, 2004). Furthermore, in a model of optic nerve injury

established by microsurgery in cats, Yu and Zhang (2011) demonstrated

immunohistochemical changes in NF, MBP, and GFAP just 3 days post-injury (Yu and

Zhang, 2011).

Given the variability in timelines for which pathological signs of optic nerve

degeneration can be observed it is possible that more delayed degeneration in the optic

nerves of TTX treated eyes could have occurred in this study. However, in keeping with most models of optic nerve degeneration, it is likely that some disruption in one of the four markers analysed in the current study would have demonstrated a change given the current timeline. Regardless, further investigations will be required into the potential long-term consequences of retinal inactivation in order to determine the safety of intraocular TTX as a potential therapy for post-critical period amblyopia.

4.6 - Limitations of immunofluorescence staining

Immunofluorescence staining was used to evaluated NF and GFAP within the optic nerves. However, this methodology has its limitations as a quantitative method. In this study we used the indirect method of immunofluorescence staining, which involves the binding of the primary antibody to the target antigen and a secondary antibody conjugated with a fluorophore that binds to the primary antibody. Although this approach allows for the amplification of the fluorescence signal which aids in visualizing the level of fluorescence. The primary and secondary antibody do not bind with a 1:1 ratio as more than one secondary antibody can bind with a primary. Furthermore, this approach does not quantify the amount of NF or GFAP within the tissue, rather, it simply allowed us to view and take a measurement of the relative amount of florescence produced. Although we were not able to quantify the amount of the protein within the tissue, we were able to compare the relative fluorescence intensity between optic nerves due to our stringent methodology. All sections were reacted on a single slide, which ensured that all sections had equal availability to the antibodies and that the tissue was reacted for the same amount of time allowing us to make the comparison of relative intensities between optic nerves.

4.7 - Anatomical changes along the optic nerve

As previously described, the anatomical characteristics of the normal optic nerve are modified along its path from optic nerve head to the optic chiasm. In the intraorbital section of the optic nerve of normal adult cats, a gradual myelination over the first 1-1.5mm of optic nerve retrolaminarly takes place, after which point the axons become uniformly myelinated (Blunt et al., 1965). In the present study, optic nerve cross-sections were taken from the first 5mm of optic nerve retrolaminarly. Therefore, it is possible that the balance in luxol staining intensity reported in this study between left (control) and right (inactivated) optic nerves in the experimental groups, may be the result of the left optic nerve section being more proximal with a naturally lower degree of myelination, and the right optic nerve section being more distal and pathologically demyelinated. However, it is unlikely that this improbable scenario occurred for all paired optic nerves. Furthermore, in this study, the luxol staining intensity observed across all sections of optic nerves examined in the experimental groups were comparable to those from controls. Therefore, it is unlikely that the balance observed in luxol staining intensity was due to pathological demyelination in TTX treated eyes.

Similarly, the fascicular structure and astrocytic distribution along the optic nerve is modified along the optic nerve pathway. In the optic nerve head, the astrocytes are bound to their extra-fascicular spaces, while in the intraorbital section of the optic nerve the number of fascicles declines and the astrocytes can be found both within and outside fascicular bundles (Triviño et al., 1996). Additionally, it was reported from longitudinally stained normal optic nerve sections in mice that there exists a slightly higher degree of GFAP immunoreactivity in the optic nerve head and first 1mm section of optic nerve

retrolaminarly in comparison to the more distal portion of the optic nerve (greater than 4mm retrolaminarly) (Cooper et al., 2018). Again, it is possible that the balance in optic nerve GFAP fluoresce intensity reported in the current study could be due to a comparison between a right more proximal section of optic nerve with a naturally occurring higher GFAP immunoreactivity, and a left more distal section with a pathological increase in GFAP immunoreactivity. Likewise, this is improbable due to the balance in staining intensity of GFAP across all sections of optic nerves examined in both the experimental and control groups reported in this study.

4.8 - The opposing pathological response of macroglia cells

In the current analyses, no difference was found in the glial cell densities between the left (control) and right (TTX treated) optic nerves across all experimental groups and controls. The measurement of glial cell density was assumed to include the quantification of both oligodendrocytes and astrocytes. Some may speculate that the balance in glial cell density between treated and control optic nerves may be due to the opposing pathological responses of macroglia cells, as the typical pattern of response of oligodendrocytes is to undergo apoptosis (Bradl and Lassmann, 2010), and alternatively, astrocytes will proliferate and be recruited to the site of injury (Eng and Ghirnikar, 1994). Therefore, it is possible that the balance in glial cell density observed in the optic nerves from the animals in the treatment groups could have been maintained even given a pathological response from macroglia cells due to a decrease in oligodendrocytes and a simultaneous and proportional increase in astrocytes. Although possible, we believe this is unlikely due to the lack of decreased luxol fast blue staining intensity as well as a lack of increased

GFAP fluorescence intensity observed in the optic nerves, suggesting that neither marker had undergone pathological modifications.

4.9 - Other potential markers of degeneration in the optic nerve

4.9.1 - Evaluation of the macroglia response

It is important to acknowledge that the current assessment of histopathology is limited to the examination of a small number of anatomical targets relative to the scope of possibilities. In the current study, the evaluation of myelin was assessed by selectively staining myelin with luxol fast blue. This has been shown to be an effective marker for demyelination in several optic nerve diseases including retinal ischemic injuries (Renner et al., 2017), glaucoma (Bordone et al., 2017), and animal models of optic neuritis (Aranda et al., 2016). In addition, oligodendrocytes, the myelinating cells of the CNS were likely included in our assessment of glial cell density in which glial cells were made visible with Nissl stain. However, in the current analyses, oligodendrocytes were not targeted specifically. Oligodendrocytes can be examined through several methodologies including immunohistochemically using antibodies against myelin oligodendrocyte glycoprotein (MOG) or counting oligodendrocyte transcription factor 2 (Olig2) positive cells. MOG is a protein located on the surface of myelinating oligodendrocytes and the external lamellae of the myelin sheath (Pham-Dinh et al., 1993). Decreases in MOG in the optic nerve have been shown to occur following retinal ischemic injury (Renner et al., 2017), and enucleations (Ludwin, 1990). Olig2, is present in oligodendrocyte progenitor cells, as well as in mature myelinating oligodendrocytes. Decreases in Olig2+ cells have been used to demonstrate not only a loss of oligodendrocytes but also the disability to remyelinate axons in the optic nerve following retinal ischemic injury (Renner et al.,

2017). Although no signs of demyelination were uncovered in our evaluation of luxol stained optic nerves, oligodendrocytes were not specifically targeted and may be an additional marker to be assessed in future studies in order to identity the definite response of oligodendrocytes to retinal inactivation therapy.

In addition, astrocytes were targeted via two means in the current analyses. First, they were expected to be included in the quantification of Nissl stained glial cell density. Second, astrocytes were evaluated by immunolabeling the astrocytic intermediate filament, GFAP. In several models of CNS and optic nerve injury the response of astrocytes has been assessed using various methodologies, primarily by labelling GFAP, but also by demonstrating increases in other intermediate filaments such as vimentin and nestin. Along with increases in GFAP, vimentin and nestin are known to simultaneously demonstrate increases following pathological insult (Pekny, 2001). Furthermore, it has been demonstrated that astrocyte localization and the orientation of astrocytic processes may be an early marker of optic nerve degeneration. In a mouse model of glaucoma, it was demonstrated that prior to overt axonal loss and gliosis, astrocytic processes retracted towards the peripheral edge of the optic nerve (Cooper et al., 2018). With disease progression, astrocytic processes invaded axonal bundles and lost their normal parallel orientation, both of which were shown to coincide with decreases in axonal density (Cooper et al., 2018). Additionally, following enucleation, it was shown that astrocytic processes invaded axonal bundles and created a disorganization in the normal cytoarchitecture of the optic nerve (Marques et al., 2003). The identification of astrocytic remodeling and disorganization of the optic nerve ultrastructure may provide earlier signs of optic nerve degeneration and should be considered in future investigations.

4.9.2 - Evaluation of the microglial response

Although we were able to asses some potential modifications in macroglia cells within the optic nerve both directly, by examining the approximate glial cell density in optic nerve cross-sections, and indirectly by observing myelin, the output of oligodendrocytes, and GFAP, expressed by astrocytes. Microglia, which play a specific role in the immune response as phagocytic cells were unlikely to have been included in our assessment. Unreactive microglia are smaller than macroglia cells and are unlikely to have been visible with the magnification used when assessing glial cell density. Although it has been reported that in the presence of pathology microglia expand in size as their cell bodies swell to phagocytose cellular debris (Sandell and Peters, 2002), reactive microglia are irregular in shape and contain several inclusion bodies (García-Cabezas et al., 2016). These abnormal characteristics would have likely impeded them from being counted during our quantification of glial cell density.

The extend of microglial activation in the optic nerve has been assessed and attributed to many of the degenerative processes that occur in response to a pathological insult in the CNS and optic nerve (Bordone et al., 2017; Bosco et al., 2015). Additionally, microglial activation has been shown to occur prior to detectable retinal ganglion cell loss in experimental models of glaucoma and may be an early marker of retinal and optic nerve disease (Bosco et al., 2011; Bosco et al., 2015). Both ionized calcium-binding adapter molecule 1 (Iba-1) and ED1 immunoreactivity are commonly used to detect microglia and macrophages in the optic nerve. Similarly to astrocytes, microglia (which are Iba1+) take on a reactive form in the presence of CNS injury. Activated microglia are phagocytic cells and are morphologically indistinguishable from macrophages that

53

originate from monocytes (Kullberg et al., 2001), along with macrophages, activated

microglia express a lysosomal monocyte antigen ED1 (Kullberg et al., 2001).

In a study by Bordone et al. (2017) the involvement of microglia in the optic

nerve degeneration that ensued in a model of experimental primary-open angle glaucoma

was assessed in rats following 6, and 15 weeks of increased IOP. Microglia cells were

analyzed by Iba1 and ED1 immunoreactivity. A significant increase in Iba1

immunoreactivity was detected after 6 weeks of elevated IOP, after 15 weeks, a reduction

in the relative Iba1 immunoreactivity was revealed (although, this was still significantly

higher than controls) (Bordone et al., 2017). In contrast, ED1 immunoreactivity was

increased at 6 weeks and further amplified at 15 weeks, demonstrating the activation of

microglia cells and/or the infiltration of macrophages. The increase and activation of

microglia was accompanied by simultaneous increases in GFAP immunoreactivity and

decreases in NF labelling and LFB staining. Interestingly, when rodents were treated with

minocycline, (which supresses microglial activation), it unsurprisingly prevented the

increase in Iba1 and ED1 immunoreactivity in the optic nerves, however, it also

prevented the increase in GFAP immunoreactivity and the decreases in luxol staining and

NF immunoreactivity, demonstrating the active and essential role of microglia in

processes of optic nerve degeneration (Bordone et al., 2017).

In consideration of the foregoing, the response of microglia to pathological

changes is accompanied by pathological responses by other cells in the optic nerve such

as astrogliosis and the breakdown of NFs and the myelin sheath (Ebneter et al., 2010;

Nakazawa et al., 2006; Renner et al., 2017; Zhang et al., 2010). Thus, it is unlikely that

microglia would have undergone histopathological changes in the optic nerve without a

simultaneous response from other cellular modifications that were included in the present analyses. nevertheless, in future studies, microglial activation should be assessed as a potential early marker of optic nerve degeneration.

4.9.3 - Evaluation of axonal integrity

In the present study, NF fluorescence intensity was examined in order to evaluate the integrity of the optic nerve axons in TTX treated eyes. However, the evaluation of more subtle modifications to the axonal ultrastructure were not assessed. Several studies have examined the structural integrity of optic nerve axons and surrounding cells with the use of electron microscopy (Pham-Dinh et al., 1993), which undoubtedly would uncover more subtle modifications to the axonal ultrastructure than what would have been analysed in the current study. In addition, other axonal pathological consequences may not have been evaluated. This includes the presence of shortened axons and retraction bulbs. It has been demonstrated that degenerating optic nerve axons may develop characteristic swellings at the axonal proximal stumps known as retraction bulbs, and in turn exhibit shortened axons (Noristani et al., 2016; Renner et al., 2017). The presence of retraction bulbs and shortened axons have been identified in animal models of glaucoma and retinal ischemic injury (Noristani et al., 2016; Renner et al., 2017). The evaluation of these features are achieved by examining longitudinal sections of the optic nerve labelled for phosphorylated NF. Analysing longitudinal sections of the optic nerve presents a unique opportunity to visualize the optic nerve's proximal and distal end to possibly identify shortened axons and early signs of degeneration at a single locations along the optic nerve. In contrast, the examination of cross-sectional slices of the optic nerve (as performed in the current study) allows for the

critical analyses of the fascicular structure of the optic nerve. That being said, certain features of axonal degeneration such as subtle modifications that would not have been visible with light microscopy, and the presence of shortened axons and retraction bulbs may have been excluded from the present analyses due to the applied methodology, and should be included in future studies.

4.9.4 - Evaluation of intracellular calcium

Furthermore, identifying markers of earlier pathological processes before actual degeneration has occurred in the optic nerve may be another sensitive and early marker of optic nerve disease. This may include the evaluation of intracellular calcium within the optic nerve. Increases in intracellular calcium have been implicated in several models of axonal degradation (Coleman, 2005). Such that, increases in intra-axonal calcium activates calpains to degrade axonal proteins like NFs, it has also been shown to increase autophagosomes, and may initiate reactive gliosis (Coleman, 2005; Knöferle et al., 2010). In a study by Knöferle et al. (2010), an influx in intra-axonal calcium in the optic nerve was observed just hours after optic nerve crush injury and was linked to the subsequent increase in autophagosomes. Furthermore, application of calcium ionophores (which facilitate the transport of calcium across plasma membranes, increasing intracellular calcium concentrations) enhanced the axonal degradation process in the optic nerve. Conversely, the use of calcium channel inhibitors was shown to significantly reduce the degradation process (Knöferle et al., 2010). Similar calcium-dependant mechanisms of degeneration have been associated with other retinal and optic nerve disorders including optic neuritis in experimental EAE (Das et al., 2013). Following induction of EAE, the optic nerves of rats were found to have increased intracellular calcium concentrations

which resulted in activated calpains, this subsequently increased glial cell infiltration and activation, as well as the release of proinflammatory cytokines (Das et al., 2013). Calpain inhibition was shown to reduce gliosis, inflammation and the subsequent degradation (Das et al., 2013), indicating the essential and early role of calcium and activated calpains in the degenerative processes in the optic nerve. Therefore, the evaluation intracellular calcium may enable the identification of earlier pathophysiological signs of optic nerve damage or disease.

In the current study we examined for gross histopathological changes in the optic nerves of animals treated with intraocular TTX. Although no signs of gross histopathology were observed, only a small number of markers were assessed to determine optic nerve integrity. Future studies should include the assessment of other markers of early degeneration such as the localization of astrocytes, the potential microglial response, the presence of retraction bulbs and shorten axons, changes in intracellular calcium concentrations, and more elusive changes in the nerve ultrastructure. This being said, the lack of pathological findings in the current study provides encouragement for further studies into the safety profile of intravitreal TTX as a potential treatment for post-critical period amblyopia.

4.10 - Alternate therapeutic uses of TTX

Although TTX is a potent neurotoxin and even in small doses administered systemically can be lethal, in appropriate quantities TTX has been shown to be a viable therapeutic option not only in animal studies but also in human trials. Specifically in human patients with severe cancer pain. In a phase 2, open-label, multicentre clinical trial, administration of intramuscular TTX was shown to diminish pain in doses of 30 ug

twice daily for 4 days. It was found that intramuscular TTX appeared safe, with few mild side effects (Hagen et al., 2007). In another randomized multicentre clinical trial by Hagen et al. (2008) the effects of subcutaneous TTX for moderate to severe cancer pain were examined with a parallel dosage and timeline to the previous study. The safety profile of TTX within this cohort was similar for patients with cancer pain and for normal human controls with mild sensory side effects which included tingling and numbness around the mouth and ataxia which occurred in only one patient and was reversible (Hagen et al., 2008).

Furthermore, Intramuscular TTX has also been studied for its effects on addiction management by reducing cue-induced drug cravings in heroin addicts. A single dose of 10μg of TTX did not produce any negative side effects in human patients who received intramuscular injections. With no reported cardiovascular concerns including no change in heart rate or blood pressure, and no adverse effects on respiration or cognition (Shi et al., 2009).

Not unlike botulinum toxin (Botox), which is one of the most poisonous toxins known to man and even in small doses can lead to a lethal descending paralysis of autonomic function. Botox is now a widely accepted therapy with an extensive therapeutic index. Although it has not yet been studied extensively in human patients, in appropriate quantities, TTX presents as a potentially viable therapeutic option for several clinical conditions, and it is not unconceivable that with the proper testing TTX would gain acceptance as a pharmacological treatment for a range of clinical diagnoses including amblyopia.

4.11 - Clinical implications

An effective treatment for post-critical period amblyopia such as retinal inactivation has a wide range of clinical implications. Not only does it provide a potential treatment for patients at ages in which no accepted therapy exists, it also has the potential to mitigate some of the existing concerns with traditional penalization treatments. As previously mentioned, penalization therapies are only successful if instilled during the critical period with adequate compliance from the patient (Loudon et al., 2002; Pediatric Eye Disease Investigator Group, 2002). However, compliance is relatively low and adherence is almost always less than prescribed (Pediatric Eye Disease Investigator Group, 2002, 2003; J. Wang, 2015). Retinal inactivation via intraocular injection as a therapy may eliminate some of the barriers to adequate compliance. Given the patient adheres to clinical administrations of the retinal inactivation treatments, compliance is guaranteed, and proper retinal inactivation can be assessed objectively.

In the current study, the effects of multiple intravitreal injections of TTX on the optic nerve of cats were examined and no signs of gross histopathology nor modifications to the optic nerve structure were observed. However, further investigation is required to fully understand the effects of TTX on the ocular structures and visual pathway. The potential long-term effects of TTX on the optic nerve, retina, and other ocular structures, as well as its systemic effects, will need to be thoroughly investigated. Additionally, many other considerations including the risks associated with administering the treatment will need to be evaluated before the translation of this therapy or a similar retinal inactivation treatment is possible in human amblyopes.

59

In recent years the use of intravitreal injection has gained increased acceptance for the therapeutic management of many ocular diseases, as intravitreal injection allows for maximal intraocular drug concentration while minimizing the risk of systemic toxicity (Jager et al., 2004). However, intraocular injections are not without risk, one such complication that can result in serious and permanent vision loss is endophthalmitis, which is a bacterial or fungal infection involving the vitreous or aqueous humour. In a comprehensive review by Jager et al. (2004), the prevalence of the most serious complications associated with intravitreal injections were analysed. It was determined that approximately 0.5% of all eyes given intravitreal injections resulted in endophthalmitis (Jager et al., 2004). Other potential complications included retinal detachment, uveitis, iritis, ocular hypertension, cataracts, and intraocular hemorrhages, however, these were more often associated with specific substances rather than the injection itself (Jager et al., 2004). The risk of serious adverse events following intraocular injection into the vitreous in adult humans is relatively low, however, not insignificant. Therefore, cautious injection techniques from highly skilled clinicians along with appropriate post-injection monitoring is required.

Despite the need for further investigation on the potential negative effects of TTX and the risks associated with administering the treatment, there exist several other unanswered questions in determining how retinal inactivation therapy would translate to clinical practice for the treatment of post-critical period amblyopia in humans. These include the dose and duration of retinal inactivation for effective treatment, the dose-response relationship for human amblyopia, the efficacy of the treatment on the different types and extents of amblyopia, and a thorough risk-benefit analysis.

In addition, the treatment of amblyopia in the visually mature also presents with some potential risks, as TTX may act as an anti-suppression therapy. In amblyopes, the development of suppression during visual immaturity acts as an adaptive mechanism to prevent diplopia. However if visual acuity is recovered and suppression is undermined, patients would likely experience double vision. Further investigation is required in order to determine if TTX removes the ability to suppress and whether binocular function can be re-established following the treatment of amblyopia with fellow eye TTX.

Notwithstanding the critical need for further investigation, the lack of optic nerve abnormalities observed in the current study provides encouragement for the use of retinal inactivation as an effective treatment for amblyopia, particularly at ages beyond the critical period when conventional treatment fails to yield significant visual recovery.

BIBLIOGRAPHY

Ahmed, A., Wang, L.L., Abdelmaksoud, S., Aboelgheit, A., Saeed, S., and Zhang, C.L. (2017). Minocycline modulates microglia polarization in ischemia-reperfusion model of retinal degeneration and induces neuroprotection. *Scientific Reports*, *7*.

Alizadeh, A., Dyck, S. M., and Karimi-Abdolrezaee, S. (2015). Myelin damage and repair in pathologic CNS: Challenges and prospects. *Frontiers in Molecular Neuroscience*, *8*.

Aranda, M. L., Fleitas, M. F. G., Laurentiis, A. D., Sarmiento, M. I. K., Chianelli, M., Sande, P. H., Dorfman, D., and Rosenstein, R. E. (2016). Neuroprotective effect of melatonin in experimental optic neuritis in rats. *Journal of Pineal Research*, *60*(3), 360–372.

Awan, M., Proudlock, F. A., and Gottlob, I. (2005). A Randomized Controlled Trial of Unilateral Strabismic and Mixed Amblyopia Using Occlusion Dose Monitors to Record Compliance. *Investigative Ophthalmology and Visual Science*, *46*(4), 1435–1439.

Barry, M. F., and Ziff, E. B. (2002). Receptor trafficking and the plasticity of excitatory synapses. *Current Opinion in Neurobiology*, *12*(3), 279–286.

Bear, M. F., Connors, B. W., and Paradiso, M. A. (2016). *Neuroscience: Exploring the brain*. Philadelphia: Wolters Kluwer.

Bear, M., Kleinschmidt, A., Gu, Q., and Singer, W. (1990). Disruption of experience-dependent synaptic modifications in striate cortex by infusion of an NMDA receptor antagonist. *The Journal of Neuroscience*, *10*(3), 909–925.

Blakemore, C., and Van Sluyters, R. C. (1974). Reversal of the physiological effects of monocular deprivation in kittens: Further evidence for a sensitive period. *The Journal of Physiology*, *237*(1), 195–216.

Blunt, M. J., Wendell-Smith, C. P., and Baldwin, F. (1965). Glia-nerve fibre relationships in mammalian optic nerve. *Journal of Anatomy*, *99*, 1–11.

Bordone, M. P., Fleitas, M. F. G., Pasquini, L. A., Bosco, A., Sande, P. H., Rosenstein, R. E., and Dorfman, D. (2017). Involvement of microglia in early axoglial alterations of the optic nerve induced by experimental glaucoma. *Journal of Neurochemistry*, *142*(2), 323–337.

Bosco, A., Steele, M. R., and Vetter, M. L. (2011). Early microglia activation in a mouse model of chronic glaucoma. *Journal of Comparative Neurology*, *519*(4), 599-620.

Bosco, A., Romero, C. O., Breen, K. T., Chagovetz, A. A., Steele, M. R., Ambati, B. K., and Vetter, M. L. (2015). Neurodegeneration severity can be predicted from early microglia alterations monitored in vivo in a mouse model of chronic glaucoma. *Disease models and mechanisms*, *8*(5), 443-455.

Bradl, M., and Lassmann, H. (2010). Oligodendrocytes: Biology and pathology. *Acta Neuropathologica*, *119*(1), 37–53.

Buch, H., Vinding, T., Cour, M. L., and Nielsen, N. V. (2001). The prevalence and causes of bilateral and unilateral blindness in an elderly urban Danish population. The Copenhagen City Eye Study. *Acta Ophthalmologica Scandinavica*, *79*(5), 441–449.

Bush, T. G., Puvanachandra, N., Horner, C. H., Polito, A., Ostenfeld, T., Svendsen, C. N., Mucke, L., Johnson, M. H., and Sofroniew, M. V. (1999). Leukocyte infiltration, neuronal degeneration, and neurite outgrowth after ablation of scar-forming, reactive astrocytes in adult transgenic mice. *Neuron*, *23*(2), 297–308.

Butt, A. M., Colquhoun, K., Tutton, M., and Berry, M. (1994). Three-dimensional morphology of astrocytes and oligodendrocytes in the intact mouse optic nerve. *Journal of Neurocytology*, *23*(8), 469–485.

Calkins, D. J. (2012). Critical pathogenic events underlying progression of neurodegeneration in glaucoma. *Progress in Retinal and Eye Research*, *31*(6), 702–719.

Castoldi, V., Marenna, S., d'Isa, R., Huang, S.-C., De Battista, D., Chirizzi, C., Chaabane, L., Kumar, D., Boschert, U., Comi, G., and Leocani, L. (2020). Non-invasive visual evoked potentials to assess optic nerve involvement in the dark agouti rat model of experimental autoimmune encephalomyelitis induced by myelin oligodendrocyte glycoprotein. *Brain Pathology*, *30*(1), 137–150.

Chen, L., Yang, C., and Mower, G. D. (2001). Developmental changes in the expression of GABAA receptor subunits (α1, α2, α3) in the cat visual cortex and the effects of dark rearing. *Molecular Brain Research*, *88*(1), 135–143.

Chen, W. S., and Bear, M. F. (2007). Activity-dependent regulation of NR2B translation contributes to metaplasticity in mouse visual cortex. *Neuropharmacology*, *52*(1).

Cho, K. K. A., Khibnik, L., Philpot, B. D., and Bear, M. F. (2009). The ratio of NR2A/B NMDA receptor subunits determines the qualities of ocular dominance plasticity in visual cortex. *Proceedings of the National Academy of Sciences of the United States of America*, *106*(13), 5377–5382.

Coleman, J. E., Nahmani, M., Gavornik, J. P., Haslinger, R., Heynen, A. J., Erisir, A., and Bear, M. F. (2010). Rapid Structural Remodeling of Thalamocortical Synapses Parallels Experience-Dependent Functional Plasticity in Mouse Primary Visual Cortex. *The Journal of Neuroscience*, *30*(29), 9670–9682.

Coleman, M. (2005). Axon degeneration mechanisms: Commonality amid diversity. *Nature Reviews. Neuroscience*, *6*(11), 889–898.

Cooper, L. N., and Bear, M. F. (2012). The BCM theory of synapse modification at 30: Interaction of theory with experiment. *Nature Reviews. Neuroscience*, *13*(11), 798–810.

Cooper, M. L., Collyer, J. W., and Calkins, D. J. (2018). Astrocyte remodeling without gliosis precedes optic nerve Axonopathy. *Acta Neuropathologica Communications*, *6*.

Cottee, L. J., FitzGibbon, T., Westland, K., and Burke, W. (1991). Long Survival of Retinal Ganglion Cells in the Cat After Selective Crush of the Optic Nerve. *European Journal of Neuroscience*, *3*(12), 1245–1254.

Cragg, B., Anker, R., and Wan, Y. K. (1976). The effect of age on the reversibility of cellular atrophy in the LGN of the cat following monocular deprivation: A test of two hypotheses about cell growth. *Journal of Comparative Neurology*, *168*(3), 345–353.

Crish, Samuel D., Sappington, R. M., Inman, D. M., Horner, P. J., Calkins, D. J., and Dowling, J. E. (2010). Distal axonopathy with structural persistence in glaucomatous neurodegeneration. *Proceedings of the National Academy of Sciences of the United States of America*, *107*(11), 5196–5201.

Das, A., Guyton, M. K., Smith, A., Wallace, G., McDowell, M. L., Matzelle, D. D., Ray, S. K., and Banik, N. L. (2013). Calpain inhibitor attenuated optic nerve damage in acute optic neuritis in rats. *Journal of Neurochemistry*, *124*(1), 133–146.

Diem, R., Demmer, I., Boretius, S., Merkler, D., Schmelting, B., Williams, S. K., Sättler, M. B., Bähr, M., Michaelis, T., Frahm, J., Brück, W., and Fuchs, E. (2008). Autoimmune Optic Neuritis in the Common Marmoset Monkey: Comparison of Visual Evoked Potentials with MRI and Histopathology. *Investigative Ophthalmology and Visual Science*, *49*(8),

Dixon-Woods, M., Awan, M., and Gottlob, I. (2006). Why is compliance with occlusion therapy for amblyopia so hard? A qualitative study. *Archives of Disease in Childhood*, *91*(6), 491–494.

64

Dubový, P., Jančálek, R., and Kubek, T. (2013). Role of Inflammation and Cytokines in Peripheral Nerve Regeneration. In *International Review of Neurobiology* (Vol. 108, pp. 173–206). Elsevier.

Duffy, K. R., Fong, M., Mitchell, D. E., and Bear, M. F. (2018). Recovery from the anatomical effects of long-term monocular deprivation in cat lateral geniculate nucleus. *Journal of Comparative Neurology*, *526*(2), 310–323.

Dyck, P. J., Windebank, A. J., Low, P. A., and Baumann, W. J. (1980). Blood Nerve Barrier in Rat and Cellular Mechanisms of Lead-induced Segmental Demyelination. *Journal of Neuropathology and Experimental Neurology*, *39*(6), 700–709.

Ebneter, A., Casson, R. J., Wood, J. P. M., and Chidlow, G. (2010). Microglial Activation in the Visual Pathway in Experimental Glaucoma: Spatiotemporal Characterization and Correlation with Axonal Injury. *Investigative Ophthalmology and Visual Science*, *51*(12), 6448–6460.

Eng, L. F., and Ghirnikar, R. S. (1994). GFAP and Astrogliosis. *Brain Pathology*, *4*(3), 229–237.

Evans, A., and Jeffery, G. (1992). The fascicular organisation of the cat optic nerve. *Experimental Brain Research*, *91*(1), 79–84.

Fagiolini, M., Fritschy, J.-M., Löw, K., Möhler, H., Rudolph, U., and Hensch, T. K. (2004). Specific GABAA Circuits for Visual Cortical Plasticity. *Science*, *303*(5664), 1681–1683.

Fagiolini, M., and Hensch, T. K. (2000). Inhibitory threshold for critical-period activation in primary visual cortex. *Nature; London*, *404*(6774), 183–186.

Felten, D. L., O'Banion, M. K., and Maida, M. S. (2016). 1—Neurons and Their Properties. In D. L. Felten, M. K. O'Banion, and M. S. Maida (Eds.), *Netter's Atlas of Neuroscience (Third Edition)* (pp. 1–42). Elsevier.

Fong, M., Mitchell, D. E., Duffy, K. R., and Bear, M. F. (2016). Rapid recovery from the effects of early monocular deprivation is enabled by temporary inactivation of the retinas. *Proceedings of the National Academy of Sciences*, *113*(49), 14139–14144.

Freeman, R. D., and Olson, C. (1982). Brief periods of monocular deprivation in kittens: Effects of delay prior to physiological study. *Journal of Neurophysiology*, *47*(2), 139–150.

Friedman, S., and Shatz, C. J. (1990). The Effects of Prenatal Intracranial Infusion of Tetrodotoxin on Naturally Occurring Retinal Ganglion Cell Death and Optic Nerve Ultrastructure. *European Journal of Neuroscience*, *2*(3), 243–253.

Gallego, B. I., Salazar, J. J., de Hoz, R., Rojas, B., Ramírez, A. I., Salinas-Navarro, M., Ortín-Martínez, A., Valiente-Soriano, F. J., Avilés-Trigueros, M., Villegas-Perez, M. P., Vidal-Sanz, M., Triviño, A., and Ramírez, J. M. (2012). IOP induces upregulation of GFAP and MHC-II and microglia reactivity in mice retina contralateral to experimental glaucoma. *Journal of Neuroinflammation*, *9*(1), 92.

García-Cabezas, M. Á., John, Y. J., Barbas, H., and Zikopoulos, B. (2016). Distinction of Neurons, Glia and Endothelial Cells in the Cerebral Cortex: An Algorithm Based on Cytological Features. *Frontiers in Neuroanatomy*, *10*, 107.

Griffin, J. W., George, E. B., Hsieh, S.-T., and Glass, J. D. (1995). *Axonal degeneration and disorders of the axonal cytoskeleton*. Oxford University Press.

Guillery, R. W., and Stelzner, D. J. (1970). The differential effects of unilateral lid closure upon the monocular and binocular segments of the dorsal lateral geniculate nucleus in the cat. *Journal of Comparative Neurology*, *139*(4), 413–421.

Hadfield, T. L., McEvoy, P., Polotsky, Y., Tzinserling, V. A., and Yakovlev, A. A. (2000). The Pathology of Diphtheria. *The Journal of Infectious Diseases*, *181*(1), 116–120.

Hagen, N. A., du Souich, P., Lapointe, B., Ong-Lam, M., Dubuc, B., Walde, D., Love, R., and Ngoc, A. H. (2008). Tetrodotoxin for Moderate to Severe Cancer Pain: A Randomized, Double Blind, Parallel Design Multicenter Study. *Journal of Pain and Symptom Management*, *35*(4), 420–429.

Hagen, N. A., Fisher, K. M., Lapointe, B., Souich, P. du, Chary, S., Moulin, D., Sellers, E., and Ngoc, A. H. (2007). An Open-Label, Multi-Dose Efficacy and Safety Study of Intramuscular Tetrodotoxin in Patients with Severe Cancer-Related Pain. *Journal of Pain and Symptom Management*, *34*(2), 171–182.

Hebb, D. O. (1949). *The organization of behavior: a neuropsychological theory*. J. Wiley; Chapman and Hall.

Henkind, P. (1966). The retinal vascular system of the domestic cat. *Experimental Eye Research*, *5*(1), 10–20.

Hensch, T. K., Fagiolini, M., Mataga, N., Stryker, M. P., Baekkeskov, S., and Kash, S. F. (1998). Local GABA circuit control of experience-dependent plasticity in developing visual cortex. *Science. 282*(5393), 1504–1508.

Hensch, Takao K. (2005). Critical period plasticity in local cortical circuits. *Nature Reviews. Neuroscience*, *6*(11), 877–888.

Hensch, T. K., and Fagiolini, M. (2005). Excitatory–inhibitory balance and critical period plasticity in developing visual cortex. *Progress in brain research*, *147*, 115-124.

Hernandez, M. R., Miao, H., and Lukas, T. (2008). Astrocytes in glaucomatous optic neuropathy. *Progress in brain research*, *173*, 353-373.

Hess, R. F., Mansouri, B., and Thompson, B. (2010). A new binocular approach to the treatment of Amblyopia in adults well beyond the critical period of visual development. *Restorative Neurology and Neuroscience*, *28*(6), 793–802.

Hoffman, R. S., and Fine, I. H. (1997). Transient no light perception visual acuity after intracameral lidocaine injection. *Journal of Cataract and Refractive Surgery*, *23*(6), 957–958.

Hol, E. M., and Pekny, M. (2015). Glial fibrillary acidic protein (GFAP) and the astrocyte intermediate filament system in diseases of the central nervous system. *Current Opinion in Cell Biology*, *32*, 121–130.

Holmes, J. M., Lazar, E. L., Melia, B. M., Astle, W. F., Dagi, L. R., Donahue, S. P., Frazier, M. G., Hertle, R. W., Repka, M. X., Quinn, G. E., and Weise, K. K. (2011). Effect of age on response to amblyopia treatment in children. *Archives of Ophthalmology*, *129*(11), 1451–1457.

Holmes, J. M., and Levi, D. M. (2018). Treatment of amblyopia as a function of age. *Visual Neuroscience*, *35*.

Holmes, J. M., Manny, R. E., Lazar, E. L., Birch, E. E., Kelly, K. R., Summers, A. I., Martinson, S. R., Raghuram, A., Colburn, J. D., Law, C., Marsh, J. D., Bitner, D. P., Kraker, R. T., and Wallace, D. K. (2019). A Randomized Trial of Binocular Dig Rush Game Treatment for Amblyopia in Children Aged 7 to 12 Years of Age. *Ophthalmology*, *126*(3), 456–466.

Howell, G. R., Soto, I., Libby, R. T., and John, S. W. M. (2013). Intrinsic axonal degeneration pathways are critical for glaucomatous damage. *Experimental Neurology*, *246*, 54–61.

Hubel, D. H., and Wiesel, T. N. (1962). Receptive fields, binocular interaction and functional architecture in the cat's visual cortex. *The Journal of Physiology*, *160*(1), 106-154.2.

Hubel, D. H., and Wiesel, T. N. (1970). The period of susceptibility to the physiological effects of unilateral eye closure in kittens. *The Journal of Physiology*, *206*(2), 419–436.

Hubel, D., and Wiesel, T. (1963). Receptive fields of cells in striate cortex of very young, visually inexperienced kittens. *Journal of Neurophysiology*, *26*(6), 994–1002.

Hubel, D., and Wiesel, T. (1965). Receptive fields and functional architecture in two nonstriate visual areas (18 and 19) of the cat. *Journal of Neurophysiology*, *28*(2), 229–289.

Hubel, D., Wiesel, T., and LeVay, S. (1977). Plasticity of Ocular Dominance Columns in Monkey Striate Cortex. *Philosophical Transactions of the Royal Society of London. Series B, Biological Sciences*, *278*(961), 377–409.

Jager, R. D., Aiello, L. P., Patel, S. C., and Cunningham, E. T. (2004). Risks of intravitreous injection: A comprehensive review. *Retina, 24*(5), 676–698.

Jeffery, G. (1996). PNS features of rodent optic nerve axons. *The Journal of Comparative Neurology*, *366*(2), 370–378.

Jeffery, G., Evans, A., Albon, J., Duance, V., Neal, J., and Dawidek, G. (1995). The human optic nerve: Fascicular organisation and connective tissue types along the extra-fascicular matrix. *Anatomy and Embryology*, *191*(6), 491–502.

Jeyarasasingam, G., Snider, C. J., Ratto, G.-M., and Chalupa, L. M. (1998). Activity-regulated cell death contributes to the formation of ON and OFF α ganglion cell mosaics. *Journal of Comparative Neurology*, *394*(3), 335–343.

Johnson, R. T., and Griffin, D. E. (1987). Postinfectious encephalomyelitis. In *Infections of the nervous system*. 209-226. Butterworth-Heinemann.

Jones, R. S., Minogue, A. M., Connor, T. J., and Lynch, M. A. (2013). Amyloid-β-Induced Astrocytic Phagocytosis is Mediated by CD36, CD47 and RAGE. *Journal of Neuroimmune Pharmacology*, *8*(1), 301–311.

Kelly, K. R., Jost, R. M., Dao, L., Beauchamp, C. L., Leffler, J. N., and Birch, E. E. (2016). Binocular iPad Game vs Patching for Treatment of Amblyopia in Children: A Randomized Clinical Trial. *JAMA Ophthalmology*, *134*(12), 1402–1408.

Khan, A. A. (2004). Wallerian Degeneration in the Optic Nerve of the Rabbit. *Cells Tissues Organs; Basel*, *177*(2), 104–109.

Kirkwood, A., Rioult, M. G., and Bear, M. F. (1996). Experience-dependent modification of synaptic plasticity in visual cortex. *Nature; London*, *381*(6582), 526–528.

Klaeger-Manzanell, C., Hoyt, C. S., and Good, W. V. (1994). Two step recovery of vision in the amblyopic eye after visual loss and enucleation of the fixing eye. *The British Journal of Ophthalmology*, *78*(6), 506–507.

Knöferle, J., Koch, J. C., Ostendorf, T., Michel, U., Planchamp, V., Vutova, P., Tönges, L., Stadelmann, C., Brück, W., Bähr, M., Lingor, P., and Nathans, J. (2010). Mechanisms of acute axonal degeneration in the optic nerve in vivo. *Proceedings of the National Academy of Sciences of the United States of America*, *107*(13), 6064–6069.

Kratz, K. E., and Spear, P. D. (1976). Postcritical-period reversal of effects of monocular deprivation on striate cortex cells in the cat. *Journal of Neurophysiology*, *39*(3), 501–511.

Kullberg, S., Aldskogius, H., and Ulfhake, B. (2001). Microglial activation, emergence of ED1-expressing cells and clusterin upregulation in the aging rat CNS, with special reference to the spinal cord. *Brain Research*, *899*(1), 169–186.

Lampert, P. W., Vogel, M. H., and Zimmerman, L. E. (1968). Pathology of the Optic Nerve in Experimental Acute Glaucoma: Electron Microscopic Studies. *Investigative Ophthalmology and Visual Science*, *7*(2), 199–213.

Lee, M. K., and Cleveland, D. W. (1996). Neuronal Intermediate Filaments. *Annual Review of Neuroscience*, *19*(1), 187–217.

LeVay, S., Wiesel, T. N., and Hubel, D. H. (1980). The development of ocular dominance columns in normal and visually deprived monkeys. *The Journal of Comparative Neurology*, *191*(1), 1–51.

Li, J., Thompson, B., Deng, D., Chan, L. Y. L., Yu, M., and Hess, R. F. (2013). Dichoptic training enables the adult amblyopic brain to learn. *Current Biology*, *23*(8), 308–309.

Lincoff, H., Zweifach, P., Brodie, S., Fuchs, W., Gross, S., Kornmehl, E., Krauss, M., Iwamoto, T., and Jakobiec, F. (1985). Intraocular injection of lidocaine. *Ophthalmology*, *92*(11), 1587–1591.

Loudon, S. E., Passchier, J., Chaker, L., Vos, S. de, Fronius, M., Harrad, R. A., Looman, C. W. N., Simonsz, B., and Simonsz, H. J. (2009). Psychological causes of non-compliance with electronically monitored occlusion therapy for amblyopia. *British Journal of Ophthalmology*, *93*(11), 1499–1503.

Loudon, S. E., Polling, J. R., and Simonsz, H. J. (2002). A preliminary report about the relation between visual acuity increase and compliance in patching therapy for amblyopia. *Strabismus*, *10*(2), 79–82.

Ludwin, S. K. (1990). Phagocytosis in the rat optic nerve following Wallerian degeneration. *Acta Neuropathologica*, *80*(3), 266–273.

69

Lüscher, C., and Malenka, R. C. (2012). NMDA Receptor-Dependent Long-Term Potentiation and Long-Term Depression (LTP/LTD). *Cold Spring Harbor Perspectives in Biology*, *4*(6).

Marques, S. A., Taffarel, M., and Blanco Martinez, A. M. (2003). Participation of neurofilament proteins in axonal dark degeneration of rat's optic nerves. *Brain Research*, *969*(1), 1–13.

May, C. A. (2008). Comparative anatomy of the optic nerve head and inner retina in non-primate animal models used for glaucoma research. *The Open Ophthalmology Journal*, *2*, 94–101.

Mayo, L., Trauger, S. A., Blain, M., Nadeau, M., Patel, B., Alvarez, J. I., Mascanfroni, I. D., Yeste, A., Kivisäkk, P., Kallas, K., Ellezam, B., Bakshi, R., Prat, A., Antel, J. P., Weiner, H. L., and Quintana, F. J. (2014). Regulation of astrocyte activation by glycolipids drives chronic CNS inflammation. *Nature Medicine; New York*, *20*(10), 1147–1156.

McBain, C. J., and Mayer, M. L. (1994). N-methyl-D-aspartic acid receptor structure and function. *Physiological Reviews*, *74*(3), 723–760.

McKee, S. P., Levi, D. M., and Movshon, J. A. (2003). The pattern of visual deficits in amblyopia. *Journal of Vision*, *3*(5), 380–405.

Miller, N. R., Johnson, M. A., Nolan, T., Guo, Y., Bernstein, A. M., and Bernstein, S. L. (2014). Sustained Neuroprotection From a Single Intravitreal Injection of PGJ2 in a Nonhuman Primate Model of Nonarteritic Anterior Ischemic Optic Neuropathy. *Investigative Ophthalmology and Visual Science*, *55*(11), 7047–7056.

Movshon, J. A. (1976). Reversal of the physiological effects of monocular deprivation in the kitten's visual cortex. *The Journal of Physiology*, *261*(1), 125–174.

Nakazawa, T., Nakazawa, C., Matsubara, A., Noda, K., Hisatomi, T., She, H., Michaud, N., Hafezi-Moghadam, A., Miller, J. W., and Benowitz, L. I. (2006). Tumor necrosis factor-alpha mediates oligodendrocyte death and delayed retinal ganglion cell loss in a mouse model of glaucoma. *Journal of Neuroscience*, *26*(49), 12633–12641.

Nase, G., Weishaupt, J., Stern, P., Singer, W., and Monyer, H. (1999). Genetic and epigenetic regulation of NMDA receptor expression in the rat visual cortex. *The European Journal of Neuroscience*, *11*(12), 4320–4326.

Newsham, D. (2000). Parental non-concordance with occlusion therapy. *British Journal of Ophthalmology*, *84*(9), 957–962.

Nguyen, J. V., Soto, I., Kim, K.-Y., Bushong, E. A., Oglesby, E., Valiente-Soriano, F. J., Yang, Z., Davis, C. O., Bedont, J. L., Son, J. L., Wei, J. O., Buchman, V. L., Zack, D. J., Vidal-Sanz, M., Ellisman, M. H., and Marsh-Armstrong, N. (2011). Myelination transition zone astrocytes are constitutively phagocytic and have synuclein dependent reactivity in glaucoma. *Proceedings of the National Academy of Sciences*, *108*(3), 1176–1181.

Noristani, R., Kuehn, S., Stute, G., Reinehr, S., Stellbogen, M., Dick, H. B., and Joachim, S. C. (2016). Retinal and Optic Nerve Damage is Associated with Early Glial Responses in an Experimental Autoimmune Glaucoma Model. *Journal of Molecular Neuroscience*, *58*(4), 470–482.

Nowak, L., Bregestovski, P., Ascher, P., Herbet, A., and Prochiantz, A. (1984). Magnesium gates glutamate-activated channels in mouse central neurones. *Nature*, *307*(5950), 462–465.

O'Callaghan, J. P. (1991). Assessment of neurotoxicity: Use of glial fibrillary acidic protein as a biomarker. *Biomedical and Environmental Sciences*, *4*(1–2), 197–206.

Ohki, K., and Reid, R. C. (2007). Specificity and randomness in the visual cortex. *Current Opinion in Neurobiology*, *17*(4), 401–407.

O'Leary, D. D., Crespo, D., Fawcett, J. W., and Cowan, W. M. (1986). The effect of intraocular tetrodotoxin on the postnatal reduction in the numbers of optic nerve axons in the rat. *Brain Research*, *395*(1), 96–103.

Olson, C. R., and Freeman, R. D. (1975). Progressive changes in kitten striate cortex during monocular vision. *Journal of Neurophysiology*, *38*(1), 26–32.

Osborne, N. N., Casson, R. J., Wood, J. P. M., Chidlow, G., Graham, M., and Melena, J. (2004). Retinal ischemia: Mechanisms of damage and potential therapeutic strategies. *Progress in Retinal and Eye Research*, *23*(1), 91–147.

Pau, D., Al Zubidi, N., Yalamanchili, S., Plant, G. T., and Lee, A. G. (2011). Optic neuritis. *Eye*, *25*(7), 833–842.

Pediatric Eye Disease Investigator Group. (2002). A randomized trial of atropine vs. Patching for treatment of moderate amblyopia in children. *Archives of Ophthalmology*, *120*(3), 268–278.

Pediatric Eye Disease Investigator Group. (2003). A randomized trial of prescribed patching regimens for treatment of severe amblyopia in children. *Ophthalmology*, *110*(11), 2075–2087.

Pekny, M. (2001). Astrocytic intermediate filaments: Lessons from GFAP and vimentin knock-out mice. *Progress in Brain Research*, *132*, 23–30.

Petzold, A. (2005). Neurofilament phosphoforms: Surrogate markers for axonal injury, degeneration and loss. *Journal of the Neurological Sciences*, *233*(1–2), 183–198.

Pham-Dinh, D., Dautigny, A., Mattei, M. G., Roeckel, N., Nussbaum, J. H., Roussel, G., Pontarotti, P., Mather, I. H., Artzt, K., and Lindahl, K. F. (1993). Myelin-oligodendrocyte glycoprotein is a member of a subset of the immunoglobulin superfamily encoded within the major histocompatibility complex. *Proceedings of the National Academy of Sciences of the United States of America*, *90*(17), 7990-7994.

Philpot, B. D., Cho, K. K. A., and Bear, M. F. (2007). Obligatory role of NR2A for metaplasticity in visual cortex. *Neuron*, *53*(4), 495–502.

Piochon, C., Kano, M., and Hansel, C. (2016). LTD-like molecular pathways in developmental synaptic pruning. *Nature Neuroscience*, *19*(10), 1299–1310.

Popescu, B. F. Gh., Pirko, I., and Lucchinetti, C. F. (2013). Pathology of Multiple Sclerosis: Where Do We Stand? *Continuum : Lifelong Learning in Neurology*, *19*(4 Multiple Sclerosis), 901–921.

Prineas, J. (1969). The pathogenesis of dying-back polyneuropathies: part II. An ultrastructural study of experimental acrylamide intoxication in the cat. *Journal of Neuropathology and Experimental Neurology*, *28*(4), 598-621.

Prineas, J. W. (1981). Pathology of the Guillain-Barré syndrome. *Annals of Neurology*, *9*(1), 6–19.

Quinlan, E. M., Philpot, B. D., Huganir, R. L., and Bear, M. F. (1999). Rapid, experience-dependent expression of synaptic NMDA receptors in visual cortex in vivo. *Nature Neuroscience*, *2*(4), 352.

Rahi, J., Logan, S., Timms, C., Russell-Eggitt, I., and Taylor, D. (2002). Risk, causes, and outcomes of visual impairment after loss of vision in the non-amblyopic eye: A population-based study. *Lancet (London, England)*, *360*(9333), 597–602.

Renner, M., Stute, G., Alzureiqi, M., Reinhard, J., Wiemann, S., Schmid, H., Faissner, A., Dick, H. B., and Joachim, S. C. (2017). Optic Nerve Degeneration after Retinal Ischemia/Reperfusion in a Rodent Model. *Frontiers in Cellular Neuroscience*, *11,* 254.

Rittenhouse, C. D., Shouval, H. Z., Paradiso, M. A., and Bear, M. F. (1999). Monocular deprivation induces homosynaptic long-term depression in visual cortex. *Nature*, *397*(6717), 347–350.

Saab, A. S., Tzvetanova, I. D., and Nave, K. A. (2013). The role of myelin and oligodendrocytes in axonal energy metabolism. *Current Opinion in Neurobiology*, *23*(6), 1065–1072.

Saggu, S. K., Chotaliya, H. P., Blumbergs, P. C., and Casson, R. J. (2010). Wallerian-like axonal degeneration in the optic nerve after excitotoxic retinal insult: An ultrastructural study. *BMC Neuroscience*, *11*(1), 97.

Salgado, C., Vilson, F., Miller, N. R., and Bernstein, S. L. (2011). Cellular Inflammation in Nonarteritic Anterior Ischemic Optic Neuropathy and Its Primate Model. *Archives of Ophthalmology*, *129*(12), 1583–1591

Sánchez, I., Hassinger, L., Sihag, R. K., Cleveland, D. W., Mohan, P., and Nixon, R. A. (2000). Local control of neurofilament accumulation during radial growth of myelinating axons in vivo. Selective role of site-specific phosphorylation. *The Journal of Cell Biology*, *151*(5), 1013–1024.

Sandell, J. H., and Peters, A. (2002). Effects of age on the glial cells in the rhesus monkey optic nerve. *Journal of Comparative Neurology*, *445*(1), 13–28.

Santucci, D., and Raghavachari, S. (2008). The Effects of NR2 Subunit-Dependent NMDA Receptor Kinetics on Synaptic Transmission and CaMKII Activation. *PLoS Computational Biology*, *4*(10).

Schaumburg, H. H., and Spencer, P. S. (1979). Clinical and Experimental Studies of Distal Axonopathy. A Frequent Form of Brain and Nerve Damage Produced by Environmental Chemical Hazards. *Annals of the New York Academy of Sciences*, *329*(1), 14–29.

Scheiman, M. M., Hertle, R. W., Beck, R. W., Edwards, A. R., Birch, E., Cotter, S. A., Crouch, E. R., Cruz, O. A., Davitt, B. V., Donahue, S., Holmes, J. M., Lyon, D. W., Repka, M. X., Sala, N. A., Silbert, D. I., Suh, D. W., Tamkins, S. M., and Pediatric Eye Disease Investigator Group. (2005). Randomized trial of treatment of amblyopia in children aged 7 to 17 years. *Archives of Ophthalmology*, *123*(4), 437–447.

Schneider, C. A., Rasband, W. S., and Eliceiri, K. W. (2012). NIH Image to ImageJ: 25 years of image analysis. *Nature Methods*, *9*(7), 671–675.

Seil, F. J. (1982). Demyelination. In *Advances in Cellular Neurobiology* (Vol. 3, pp. 235-274). Elsevier.

Serra, L., Cercignani, M., Lenzi, D., Perri, R., Fadda, L., Caltagirone, C., Macaluso, E., and Bozzali, M. (2010). Grey and White Matter Changes at Different Stages of Alzheimer's Disease. *Journal of Alzheimer's Disease*, *19*(1), 147–159.

73

Shatz, C. J., and Stryker, M. P. (1978). Ocular dominance in layer IV of the cat's visual cortex and the effects of monocular deprivation. *The Journal of Physiology*, *281*, 267–283.

Sherman, S. M., and Stone, J. (1973). Physiological normality of the retina in visually deprived cats. *Brain Research*, *60*(1), 224–230.

Shi, J., Liu, T.-T., Wang, X., Epstein, D. H., Zhao, L.-Y., Zhang, X.-L., and Lu, L. (2009). Tetrodotoxin reduces cue-induced drug craving and anxiety in abstinent heroin addicts. *Pharmacology Biochemistry and Behavior*, *92*(4), 603–607.

Shields, D. C., Tyor, W. R., Deibler, G. E., and Banik, N. L. (1998). Increased calpain expression in experimental demyelinating optic neuritis: An immunocytochemical study. *Brain Research*, *784*(1), 299–304.

Smith, D. C., Spear, P. D., and Kratz, K. E. (1978). Role of visual experience in postcritical-period reversal of effects of monocular deprivation in cat striate cortex. *Journal of Comparative Neurology*, *178*(2), 313–328.

Sofroniew, M. V. (2016). Reactive Astrocytes in Neural Repair and Protection: *The Neuroscientist*. *11*(5), 400-407

Song, S.-K., Sun, S.-W., Ju, W.-K., Lin, S.-J., Cross, A. H., and Neufeld, A. H. (2003). Diffusion tensor imaging detects and differentiates axon and myelin degeneration in mouse optic nerve after retinal ischemia. *NeuroImage*, *20*(3), 1714–1722.

Spear, P. D., and Hou, V. (1990). Retinal ganglion-cell densities and soma sizes are unaffected by long-term monocular deprivation in the cat. *Brain Research*, *522*(2), 354–358.

Stankowska, D. L., Mueller, B. H., Oku, H., Ikeda, T., and Dibas, A. (2018). Neuroprotective effects of inhibitors of acid-sensing ion channels (ASICs) in optic nerve crush model in rodents. *Current eye research*, *43*(1), 84-95.

Stassart, R. M., Möbius, W., Nave, K. A., and Edgar, J. M. (2018). The Axon-Myelin Unit in Development and Degenerative Disease. *Frontiers in Neuroscience*, *12*, 467.

Strominger, N. L., Demarest, R. J., and Laemle, L. B. (2012). Neurons and Associated Cells. In *Noback's Human Nervous System, Seventh Edition* (pp. 11-38). Humana Press, Totowa, NJ.

Sumner, A. J., and Asbury, A. K. (1975). Physiological studies of the dying-back phenomenon: muscle stretch afferents in acrylamide neuropathy. *Brain*, *98*(1), 91-100.

Thomalla, G., Glauche, V., Weiller, C., and Röther, J. (2005). Time course of wallerian degeneration after ischaemic stroke revealed by diffusion tensor imaging. *Journal of Neurology, Neurosurgery, and Psychiatry*, *76*(2), 266–268.

Tommila, V., and Tarkkanen, A. (1981). Incidence of loss of vision in the healthy eye in amblyopia. *The British Journal of Ophthalmology*, *65*(8), 575–577.

Triviño, A., Ramírez, J. M., Salazar, J. J., Ramírez, A. I., and García-Sánchez, J. (1996). Immunohistochemical study of human optic nerve head astroglia. *Vision Research*, *36*(14), 2015–2028.

van Leeuwen, R., Eijkemans, M. J. C., Vingerling, J. R., Hofman, A., de Jong, P. T. V. M., and Simonsz, H. J. (2007). Risk of bilateral visual impairment in individuals with amblyopia: The Rotterdam study. *The British Journal of Ophthalmology*, *91*(11), 1450–1451.

von Noorden, G. K. (1973). Histological Studies of the Visual System in Monkeys with Experimental Amblyopia. *Investigative Ophthalmology and Visual Science*, *12*(10), 727–738.

von Noorden, G. K. (1985). Amblyopia: A multidisciplinary approach. Proctor lecture. *Investigative Ophthalmology and Visual Science*, *26*(12), 1704–1716.

von Noorden, G. K., and Campos, E. C. (2002). *Binocular vision and ocular motility: Theory and management of strabismus* (6th ed). Mosby.

von Noorden, G. K., and Crawford, M. L. (1979). The sensitive period. *Transactions of the Ophthalmological Societies of the United Kingdom*, *99*(3), 442–446.

von Noorden, G. K., and Crawford, M. L. (1992). The lateral geniculate nucleus in human strabismic amblyopia. *Investigative Ophthalmology and Visual Science*, *33*(9), 2729–2732.

Wallace, M. P., Stewart, C. E., Moseley, M. J., Stephens, D. A., and Fielder, A. R. (2013). Compliance With Occlusion Therapy for Childhood Amblyopia. *Investigative Ophthalmology and Visual Science*, *54*(9), 6158–6166.

Waller, A. V., and Owen, R. (1851). Experiments on the section of the glossopharyngeal and hypoglossal nerves of the frog, and observations of the alterations produced thereby in the structure of their primitive fibres. *Abstracts of the Papers Communicated to the Royal Society of London*, *5*, 924–925.

Wang, J. (2015). Compliance and patching and atropine amblyopia treatments. *Vision Research*, *114*, 31–40.

Wang, J. C., and Shuba, L. M. (2014). A case of an adult regaining vision in the amblyopic eye. *Canadian Journal of Ophthalmology*, *49*(2), 46–48.

Wang, M.-S., Wu, Y., Culver, D. G., and Glass, J. D. (2000). Pathogenesis of Axonal Degeneration: Parallels Between Wallerian Degeneration and Vincristine Neuropathy. *Journal of Neuropathology and Experimental Neurology*, *59*(7), 599–606.

Warden, P., Bamber, N. I., Li, H., Esposito, A., Ahmad, K. A., Hsu, C. Y., and Xu, X. M. (2001). Delayed Glial Cell Death Following Wallerian Degeneration in White Matter Tracts after Spinal Cord Dorsal Column Cordotomy in Adult Rats. *Experimental Neurology*, *168*(2), 213–224.

Wiesel, T. N., and Hubel, D. H. (1963a). Single-cell responses in striate cortex of kittens deprived of vision in one eye. *Journal of neurophysiology*, *26*(6), 1003-1017.

Wiesel, T. N., and Hubel, D. H. (1963b). Effects of Visual Deprivation on Morphology and Physiology of Cells in the Cat's Lateral Geniculate Body. *Journal of Neurophysiology*, *26*(6), 978–993.

Williams, R. W., Bastiani, M. J., Lia, B., and Chalupa, L. M. (1986). Growth cones, dying axons, and developmental fluctuations in the fiber population of the cat's optic nerve. *Journal of Comparative Neurology*, *246*(1), 32–69.

Wisniewski, H. M., and Bloom, B. R. (1975). Primary demyelination as a nonspecific consequence of a cell-mediated immune reaction. *The Journal of Experimental Medicine*, *141*(2), 346–359.

Wong, V. G., and Macri, F. J. (1964). Vasculature of the cat eye. *Archives of Ophthalmology*, *72*, 351–358.

Wong-Riley, M., and Carroll, E. W. (1984). Effect of impulse blockage on cytochrome oxidase activity in monkey visual system. *Nature*, *307*(5948), 262–264.

Wong-Riley, M., and Riley, D. A. (1983). The effect of impulse blockage on cytochrome oxidase activity in the cat visual system. *Brain research*, *261*(2), 185-193.

Wright, K. W. (2003). Visual Development and Amblyopia. *Handbook of Pediatric Strabismus and Amblyopia*, 151–171.

Wu, C., and Hunter, D. G. (2006). Amblyopia: Diagnostic and Therapeutic Options. *American Journal of Ophthalmology*, *141*(1), 175-184.

Wu, G. F., Parker Harp, C. R., and Shindler, K. S. (2015). Optic Neuritis: A Model for the Immuno-pathogenesis of Central Nervous System Inflammatory Demyelinating Diseases. *Current Immunology Reviews*, *11*(2), 85–92.

Yu, F., and Zhang, R. (2011). A novel model of optic nerve injury established by microsurgery using the pterional approach in cats. *Neurology India; Mumbai*, *59*(3), 355–361.

Zhang, C., Guo, Y., Slater, B. J., Miller, N. R., and Bernstein, S. L. (2010). Axonal degeneration, regeneration and ganglion cell death in a rodent model of anterior ischemic optic neuropathy (rAION). *Experimental Eye Research*, *91*(2), 286–292.

Animal	Condition	Rearing	NF Intensity		Luxol Intensity		GFAP Intensity		Glial Cell Density (cells / mm²)	
			LE	RE	LE	RE	LE	RE	LE	RE
410	Normal	14wk +10day buffer RE	49.38	51.02	113.05	119.62	90.92	94.62	8497	9125
			-3.32%		-5.81%		-4.07%		-7.39%	
453	Normal	14wk +1day buffer RE	107.91	106.81	149.43	145.55	106.68	102.70	8612	8298
			1.02%		2.60%		3.73%		3.65%	
466	Normal	40day	70.95	75.34	112.78	122.44	122.34	131.80	6370	6166
			-6.19%		-8.57%		-7.73%		3.20%	
468	Normal	40day	68.13	72.01	149.95	154.12	119.88	117.46	8304	8012
			-5.69%		-2.78%		2.02%		3.52%	
442	RE TTX	6wk MD + 8day TTX	72.02	73.03	138.48	141.60	117.55	117.46	7841	7411
			-1.40%		-2.25%		0.08%		5.48%	
404	RE TTX	10wk MD + 10day TTX	117.58	116.72	126.17	135.76	135.80	136.79	7224	6998
			0.73%		-7.60%		-0.73%		3.13%	
451	RE TTX	10wk MD + 10day TTX	77.06	79.87	153.49	149.91	113.18	106.75	7802	7102
			-3.65%		2.33%		5.68%		8.97%	
377	RE TTX	14wk MD +10day TTX	102.80	104.97	152.11	159.07	99.45	109.42	7885	7830
			-2.11%		-4.58%		-10.03%		0.70%	
369	RETTX	16wk MD +10day TTX	115.89	118.33	149.19	152.45	123.31	121.80	8833	8436
			-2.11%		-2.19%		1.22%		4.49%	
368	RETTX	18wk MD + 10day TTX	79.93	80.91	129.37	117.97	106.74	105.84	7720	8199
			-1.23%		8.81%		0.84%		-6.20%	
381	RE TTX	6wk MD +10day TTX	NA		173.10	181.84	103.57	105.53	6843	7240
					-5.05%		-1.89%		-5.80%	
441	RE TTX+BV	6wk MD + 10day TTX + 20day BV	70.46	74.92	158.42	156.41	85.74	90.95	8521	8753
			-6.33%		1.27%		-6.08%		-2.72%	
412	RE TTX+BV	10wk MD + 10day TTX +20day BV	68.38	70.19	155.60	159.83	110.74	110.50	7367	6948
			-2.65%		-2.72%		0.22%		5.69%	
413	RE TTX+BV	10wk MD + 10day TTX + 10day BV	81.13	86.66	164.70	157.75	112.54	104.38	8282	7934
			-6.82%		4.22%		7.25%		4.20%	
450	RE TTX+BV	10wk MD + 10day	58.57	59.34	131.33	129.75	111.94	109.11	6645	7053

			NF (LE / RE)		Luxol (LE / RE)		GFAP (LE / RE)		Nissl (LE / RE)	
		TTX + 20day BV	-1.31%		1.20%		2.53%		-6.14%	
452	RE TTX+BV	10wk MD +10day TTX +20day BV	75.78	76.26	137.54	151.05	110.89	107.57	8596	7852
			-0.63%		-9.82%		2.99%		8.66%	
456	RE TTX+BV	15wk MD +10day TTX + 12day BV	103.67	99.70	179.13	175.84	96.21	98.52	NA	
			3.83%		1.83%		-2.40%			

Table 1. Measurements of neurofilament labeling intensity, luxol fast blue staining intensity, GFAP labeling intensity, and Nissl stained glial cell density in cross-sections of the optic nerve from the left and right eye.

For all animals MD was performed by lid suture of the left eye (LE) on postnatal day 30. All TTX injections (RETTX) were performed on the right eye (RE) immediately following the period of MD. Animals in the RETTX+ BV group were subject to a period of unobstructed binocular vision (BV) following retinal inactivation treatment. For each cell: measurements taken from the left optic nerve are on the top left, measurements taken from the right optic nerve are on the top right. The percent difference (ODI) is indicated at the bottom of each cell, and is calculated by the following metric: *(ODI) = ((LE-RE)/LE) x 100.* Intensity measurements for NF, Luxol and GFAP are the average mean grey value taken from 5 images from each optic nerve. NA indicates that the reaction product was not suitable for measurement.
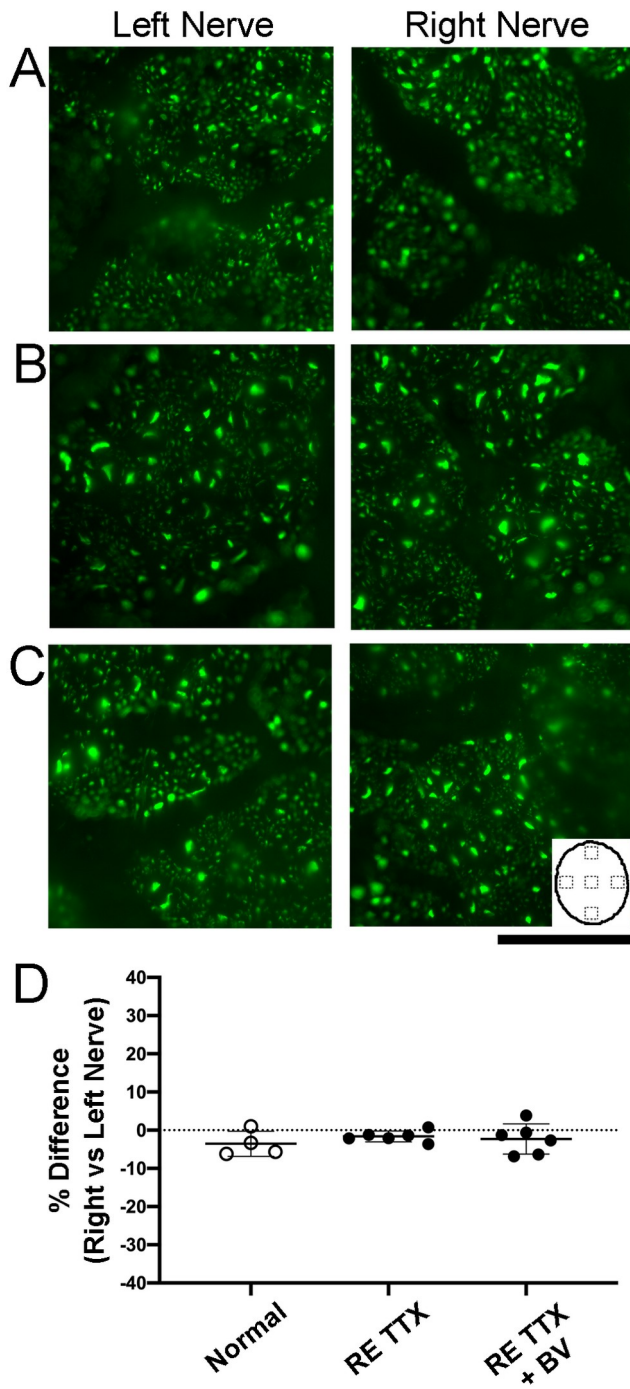
Figure 1. Examination of cross-sections of optic nerve from the left and right eye labelled for neurofilament.

For animals reared binocularly (Normals), NF labeling intensity, and distribution in the left and right optic nerves appeared balanced (A). animals that received MD followed by retinal inactivation of the fellow eye (RETTX) also showed comparable levels of NF labelling intensity in left and right optic nerves (B) which were indistinguishable from controls. NF labelling intensity from the left and right optic nerve cross-sections from animals who received up to 20 days of binocular vision following retinal inactivation treatment (RETTX+BV) showed comparable staining intensities (C) and were likewise similar to controls. The inset in C demonstrates the approximate location of the 5 images captured from which measurement were taken for each optic nerve cross-section. The percentage difference in NF labelling intensity between the left and right optic nerve for each animal revealed minor differences indicated by ODI values close to zero for all animals across all treatment groups (D) which were not found to be significantly different between treatment groups (H=[3] = 0.76, p=0.71; Dunn's multiple comparison test: p > 0.05). Scale bar = 250 microns.
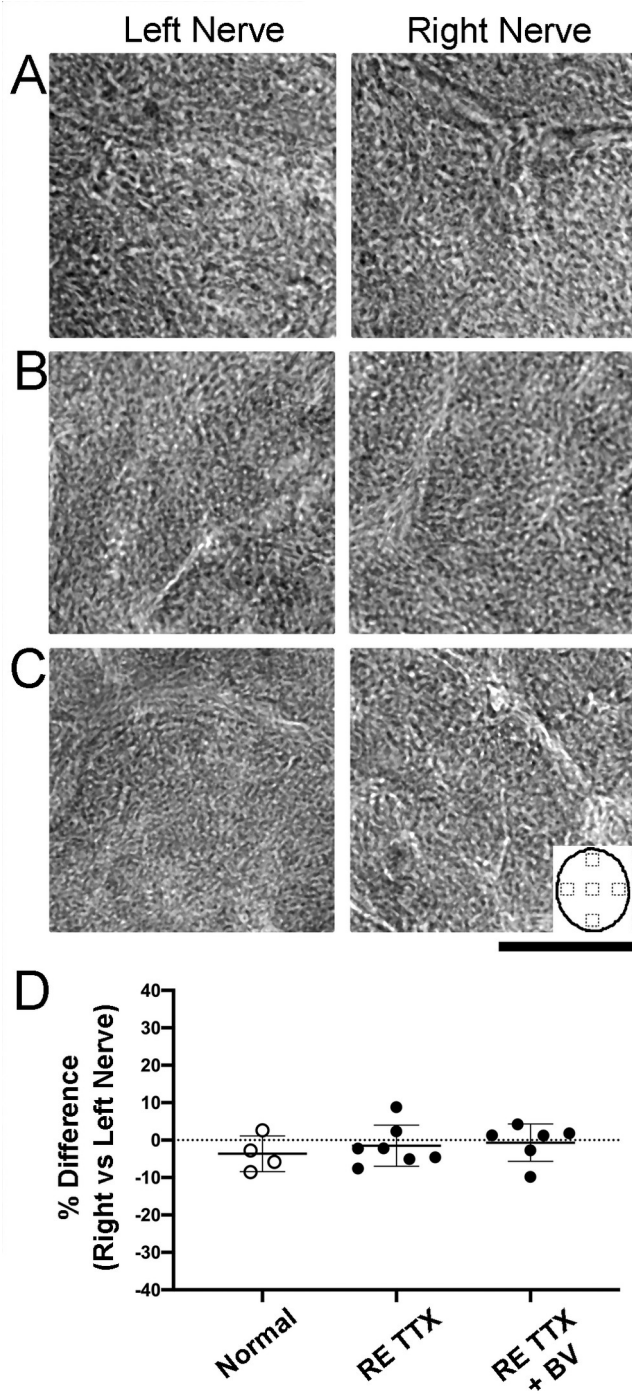
Figure 2. Examination of cross-sections of optic nerve from the left and right eye stained with luxol fast blue to evaluate myelin.

The myelin staining intensity appeared to be balanced between the left and right

optic nerves of animals in the normal control group (A). Animals from the RETTX group

showed balanced staining intensities between the left and right eye which were similar to controls (B). Moreover, animals in the RETTX+BV treatment group also showed a comparable level of staining intensity between left and right optic nerves which were also indistinguishable from controls (C). The inset in C demonstrates the approximate location of the 5 images captured from which measurement were taken for each optic nerve cross-section. The ODI values for animals in the Normal group and both treatment groups (RETTX and RETTX+BV) were similar (D) and were not found to be statistically different (H=[3] = 0.95, p = 0.64; Dunn's multiple comparison test: p > 0.05). Scale bar = 250 microns.
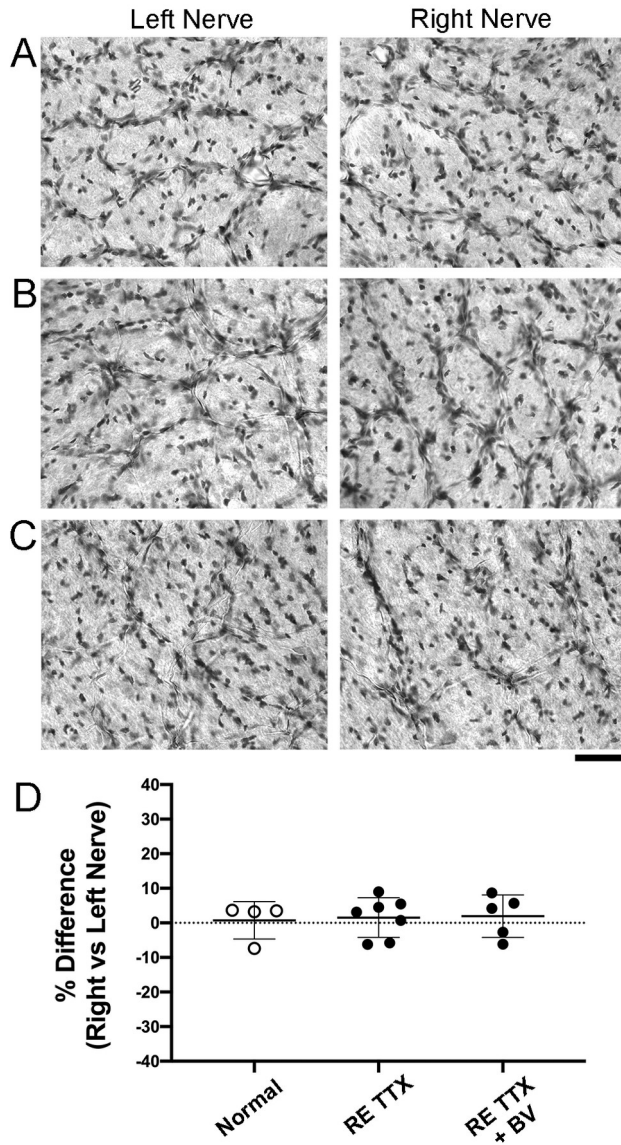
Figure 3. Nissl stained cross-sections of optic nerve from the left and right eye for the quantification of glial cell density.

Quantification of glial cell density revealed a balance in glial cells between the left and right optic nerves of control animals (A). likewise, glial cell densities were similar between the left and right optic nerves of animals subject to up to 10 days of retinal inactivation (B) which was comparable to controls. Furthermore, animals given a period of up to 20 days of binocular vision following retinal inactivation had similar glial cell densities between left and right optic nerves (C) and were also similar to controls.

ODIs across groups revealed similar minor differences in glial cell densities (D) which

were not significantly different (H=[3] = 0.67, p = 0.74; Dunn's multiple comparison test:
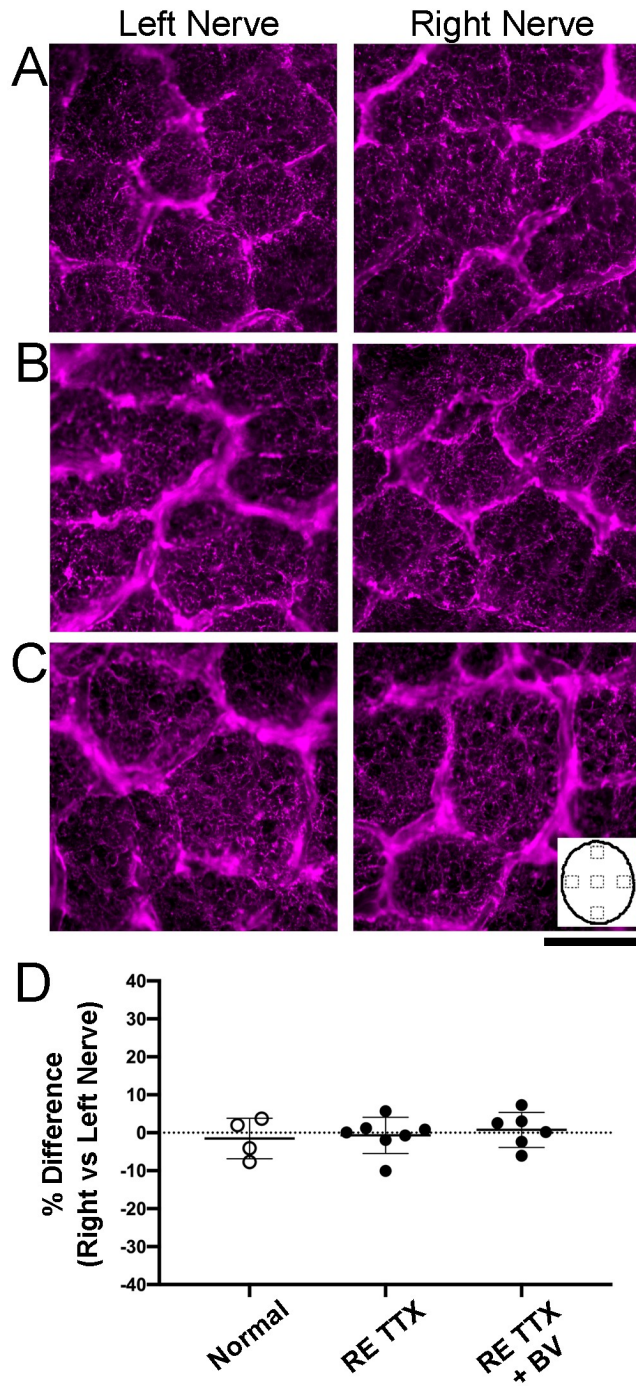
p > 0.05). Scale bar = 50 microns.

Figure 4. Examination of cross-sections of optic nerve from the left and right eye labelled for GFAP.

GFAP labelling intensity was similar between the left and right optic nerves of control animals (A). Similar labelling intensities were also appreciated between the left and right optic nerves of animals in both treatment groups (B and C) which were likewise

similar to controls. The inset in C demonstrates the approximate location of the 5 images captured from which measurement were taken from each optic nerve cross-section. ODI values were similar for all animals across groups (D) and were not found to be significantly different (H=[3] = 0.49, p = 0.79; Dunn's multiple comparison test: p > 0.05). Scale bar = 250 microns.